Consistent satellite XCO2 retrievals from SCIAMACHY and GOSAT using the BESD algorithm

J. Heymann, M. Reuter, M. Hilker, M. Buchwitz, O. Schneising, H. Bovensmann, J. P. Burrows, A. Kuze, H. Suto, N. M. Deutscher, M. K. Dubey, D. W. T. Griffith, F. Hase, S. Kawakami, R. Kivi, I. Morino, C. Petri, C. Roehl, M. Schneider, V. Sherlock, Ralf Sussmann, V. A. Velazco, T. Warneke, D. Wunch

Angaben zur Veröffentlichung / Publication details:

Heymann, J., M. Reuter, M. Hilker, M. Buchwitz, O. Schneising, H. Bovensmann, J. P. Burrows, et al. 2015. “Consistent satellite XCO2 retrievals from SCIAMACHY and GOSAT using the BESD algorithm.” Atmospheric Measurement Techniques 8 (7): 2961–80. https://doi.org/10.5194/amt-8-2961-2015.

Atmos. Meas. Tech., 8, 2961–2980, 2015
www.atmos-meas-tech.net/8/2961/2015/
doi:10.5194/amt-8-2961-2015

Atmospheric Measurement Techniques
Open Access

Consistent satellite XCO_2 retrievals from SCIAMACHY and GOSAT using the BESD algorithm

J. Heymann[1], M. Reuter[1], M. Hilker[1], M. Buchwitz[1], O. Schneising[1], H. Bovensmann[1], J. P. Burrows[1], A. Kuze[2], H. Suto[2], N. M. Deutscher[1,4], M. K. Dubey[3], D. W. T. Griffith[4], F. Hase[5], S. Kawakami[2], R. Kivi[6], I. Morino[7], C. Petri[1], C. Roehl[8], M. Schneider[5], V. Sherlock[9,a], R. Sussmann[10], V. A. Velazco[4], T. Warneke[1], and D. Wunch[8]

[1]Institute of Environmental Physics (IUP), University of Bremen, Bremen, Germany
[2]Japan Aerospace Exploration Agency (JAXA), Tsukuba, Japan
[3]Los Alamos National Laboratory, Los Alamos, USA
[4]Centre for Atmospheric Chemistry, University of Wollongong, Wollongong, Australia
[5]IMK-ASF, Karlsruhe Institute of Technology (KIT), Karlsruhe, Germany
[6]Finnish Meteorological Institute, Sodankylä, Finland
[7]National Institute for Environmental Studies (NIES), Tsukuba, Japan
[8]California Institute of Technology, Pasadena, USA
[9]National Institute of Water and Atmospheric Research, Wellington, New Zealand
[10]IMK-IFU, Karlsruhe Institute of Technology (KIT), Garmisch-Partenkirchen, Germany
[a]now at: Laboratoire de Météorologie Dynamique, Palaiseau, France

Correspondence to: J. Heymann (heymann@iup.physik.uni-bremen.de)

Received: 19 December 2014 – Published in Atmos. Meas. Tech. Discuss.: 13 February 2015
Revised: 22 June 2015 – Accepted: 4 July 2015 – Published: 24 July 2015

Abstract. Consistent and accurate long-term data sets of global atmospheric concentrations of carbon dioxide (CO_2) are required for carbon cycle and climate-related research. However, global data sets based on satellite observations may suffer from inconsistencies originating from the use of products derived from different satellites as needed to cover a long enough time period. One reason for inconsistencies can be the use of different retrieval algorithms. We address this potential issue by applying the same algorithm, the Bremen Optimal Estimation DOAS (BESD) algorithm, to different satellite instruments, SCIAMACHY on-board ENVISAT (March 2002–April 2012) and TANSO-FTS on-board GOSAT (launched in January 2009), to retrieve XCO_2, the column-averaged dry-air mole fraction of CO_2. BESD has been initially developed for SCIAMACHY XCO_2 retrievals. Here, we present the first detailed assessment of the new GOSAT BESD XCO_2 product. GOSAT BESD XCO_2 is a product generated and delivered to the MACC project for assimilation into ECMWF's Integrated Forecasting System. We describe the modifications of the BESD algorithm needed in order to retrieve XCO_2 from GOSAT and present detailed comparisons with ground-based observations of XCO_2 from the Total Carbon Column Observing Network (TCCON). We discuss detailed comparison results between all three XCO_2 data sets (SCIAMACHY, GOSAT and TCCON). The comparison results demonstrate the good consistency between SCIAMACHY and GOSAT XCO_2. For example, we found a mean difference for daily averages of -0.60 ± 1.56 ppm (mean difference $\pm$ standard deviation) for GOSAT–SCIAMACHY (linear correlation coefficient $r = 0.82$), -0.34 ± 1.37 ppm ($r = 0.86$) for GOSAT–TCCON and 0.10 ± 1.79 ppm ($r = 0.75$) for SCIAMACHY–TCCON. The remaining differences between GOSAT and SCIAMACHY are likely due to non-perfect collocation (± 2 h, $10^\circ \times 10^\circ$ around TCCON sites), i.e. the observed air masses are not exactly identical but likely also due to a still non-perfect BESD retrieval algorithm, which will be continuously improved in the future. Our overarching goal is to generate a satellite-derived XCO_2 data set appropriate for climate and carbon cycle research covering the longest possible time period. We therefore also plan to extend the existing SCIAMACHY and

GOSAT data set discussed here by also using data from other missions (e.g. OCO-2, GOSAT-2, CarbonSat) in the future.

1 Introduction

Space-based observations of carbon dioxide (CO_2) can contribute to the elimination of important knowledge gaps related to the regional sources and sinks of CO_2 (Rayner and O'Brien, 2001; Hungershoefer et al., 2010; Schneising et al., 2013, 2014; Reuter et al., 2014b, c). Near-surface sensitive measurements of column-averaged dry-air mole fractions of CO_2 (XCO_2) in the short-wave infrared spectral region (SWIR) are well suited for this application. These observations can complement measurements from existing surface-based greenhouse gas monitoring networks, especially in data-poor regions, by providing data with dense spatial coverage. However, satellite measurements need to be precise and accurate enough to reduce uncertainties in the characterisation of the sources and sinks. Studies showed that a precision of better than 1 % for regional averages and monthly means (Rayner and O'Brien, 2001; Houweling et al., 2004) and regional biases of less than a few tenth of a part per million (ppm) are required (Chevallier et al., 2007; Miller et al., 2007).

The SCanning Imaging Absorption spectroMeter for Atmospheric CHartographY (SCIAMACHY) on-board the European Space Agency's (ESA) Environmental Satellite (ENVISAT) (Burrows et al., 1995; Bovensmann et al., 1999), launched in 2002, was in the time period before mid-2009 the only satellite instrument measuring XCO_2 with high surface sensitivity. The long-term time series of surface-sensitive satellite-derived XCO_2 starts with SCIAMACHY. SCIAMACHY had observed the Earth's atmosphere until the loss of ENVISAT in April 2012.

The Thermal And Near infrared Sensor for carbon Observations Fourier Transform Spectrometer (TANSO-FTS) on-board the Greenhouse gases Observing SATellite (GOSAT) (Kuze et al., 2009), launched in January 2009, and the Orbiting Carbon Observatory-2 (OCO-2) (Crisp et al., 2004), launched in July 2014, are currently the only satellite instruments yielding XCO_2 with high near-surface sensitivity. Both satellite missions are specifically designed to observe XCO_2.

Several retrieval algorithms have been developed to evaluate the satellite observations for SCIAMACHY (e.g. Schneising et al., 2012; Heymann et al., 2012b; Reuter et al., 2011) and for GOSAT (e.g. Yoshida et al., 2013; Crisp et al., 2012; Guerlet et al., 2013; Cogan et al., 2012; Oshchepkov et al., 2008). These algorithms differ e.g. in cloud and aerosol treatment, state vector elements and cloud filtering (for more details see, e.g. Reuter et al., 2013; Takagi et al., 2014). One of these algorithms is the Bremen Optimal Estimation DOAS (BESD) retrieval algorithm developed for the evaluation of SCIAMACHY measurements at the University of Bremen (Reuter et al., 2010, 2011). As unaccounted scattering by aerosols and clouds is a major error source for satellite retrievals (e.g. Aben et al., 2006; Houweling et al., 2005; Heymann et al., 2012a; Guerlet et al., 2013), BESD aims to reduce this error source by explicitly considering atmospheric scattering (Reuter et al., 2010). The BESD algorithm has been used to generate a SCIAMACHY XCO_2 data product ranging from 2002 to 2012. This data product has been used in several key European projects, e.g. ESA's Climate Change Initiative (CCI, www.esa-ghg-cci.org and Buchwitz et al., 2013b; Hollmann et al., 2013) and the EU's Monitoring of Atmospheric Composition and Climate (MACC, Hollingsworth et al., 2008) project.

Carbon cycle and climate-related research requires consistent and accurate long-term global CO_2 data sets. However, global data sets based on observations from different satellite instruments may suffer from inconsistencies originating from the use of different satellite algorithms. We address this potential issue by applying the same retrieval algorithm, the BESD algorithm, to different satellite instruments, SCIAMACHY and TANSO-FTS. Within the European MACC project, after the loss of ENVISAT, the BESD algorithm has been modified to also retrieve XCO_2 from TANSO-FTS measurements. The GOSAT/TANSO-FTS BESD XCO_2 product was delivered for the assimilation into the European Centre for Medium-range Weather Forecasts (ECMWF) Integrated Forecasting System (Agustí-Panareda et al., 2014). Here, we report first results of an assessment of the new GOSAT BESD XCO_2 data product. In addition, we discuss results of an investigation concerning the consistency of the SCIAMACHY BESD and GOSAT BESD XCO_2 data sets. This analysis includes a comparison of validation results obtained by using data from the Total Carbon Column Observing Network (TCCON, Wunch et al., 2011a), a direct comparison of daily satellite-based XCO_2 data and a global comparison with NOAA's CO_2 modelling and assimilation system CarbonTracker (Peters et al., 2007).

This paper is structured as follows: in Sects. 2 and 3, relevant aspects of the SCIAMACHY and TANSO-FTS instruments are discussed. Section 4 gives a short overview of the SCIAMACHY BESD retrieval algorithm whereas in Sect. 5 the recently developed GOSAT BESD XCO_2 retrieval algorithm is introduced. This includes the GOSAT Level 1C generation (fully calibrated total intensity, measurement error and a priori information), the GOSAT Level 2 XCO_2 generation as well as the cloud filtering and post-processing. In Sects. 6 and 7 the comparison of the satellite XCO_2 data with TCCON and CarbonTracker are described and discussed. Finally, conclusions are given in Sect. 8.

2 SCIAMACHY on ENVISAT

The satellite instrument SCIAMACHY (Burrows et al., 1995; Bovensmann et al., 1999) was part of the atmospheric chemistry payload on-board ESA's ENVISAT. The ENVISAT satellite was launched in March 2002. On 8 April 2012, after 10 years of operation, ESA lost contact to ENVISAT and finally had declared the official end of the ENVISAT mission on 9 May 2012. ENVISAT flew on a sun-synchronous daytime (descending) orbit with an equator crossing time of 10:00 local time (LT).

The SCIAMACHY instrument was a passive remote sensing moderate-resolution imaging spectrometer and measured sunlight transmitted, reflected and scattered by the Earth's atmosphere or surface in the ultraviolet, visible and near-infrared wavelength regions in eight spectral channels (214–1750, 1940–2040, 2265–2380 nm) with a spectral resolution between 0.2 and 1.4 nm. The scientific objective of SCIAMACHY was to improve our knowledge of global atmospheric change and related issues of importance to the chemistry and physics of the atmosphere, i.e. the impact of pollution, exchange processes between atmospheric layers, atmospheric chemistry in polar and other regions and the influence of natural phenomena such as volcanic eruptions. Targets of SCIAMACHY were atmospheric gases (e.g. O_3, NO_2, CH_4 and CO_2) as well as clouds and aerosols, ocean colour and land parameters. SCIAMACHY measured in three different viewing geometries: nadir, limb and solar/lunar occultation.

For the work presented in this study the nadir mode observations in channel 4 (755–775 nm) and channel 6 (1558–1594 nm) has been used. The integration time of the instrument in the used spectral regions was typically 0.25 s. This provided a typical spatial resolution of ~ 60 km across track and ~ 30 km along track. By scanning $\pm 32°$ across track, SCIAMACHY achieved a swath width of ~ 1000 km.

3 TANSO-FTS on GOSAT

GOSAT was the first satellite mission dedicated to measuring atmospheric XCO_2 and XCH_4 (Kuze et al., 2009). GOSAT is a joint project of the Japanese Aerospace Exploration Agency, the National Institute for Environmental Studies and the Ministry of the Environment. The objectives of GOSAT are to monitor the global distribution of greenhouse gases, to estimate CO_2 and CH_4 sources and sinks on sub-continental scale and to verify reductions of anthropogenic greenhouse gas emissions (Kuze et al., 2009). On 23 January 2009, GOSAT was launched in a sun-synchronous daytime orbit with an equator crossing time of 13:00 (LT).

GOSAT carries two satellite instruments, the TANSO-FTS and the Cloud and Aerosol Imager (TANSO-CAI). The TANSO-FTS is a double pendulum interferometer. It measures two orthogonal polarisation directions of reflected or scattered sunlight in three bands (bands 1, 2, 3) in the SWIR between 4800 and 13 200 cm^{-1} (758–2083 nm). In addition to the SWIR bands, band 4 measures in the thermal infrared between 700 and 1800 cm^{-1} (5.56–14.3 µm). However, measurements obtained with band 4 are not considered in this paper. TANSO-FTS has a spectral resolution of $\Delta\nu_1 \approx 0.36\,cm^{-1}$ ($\Delta\lambda_1 \approx 0.02$ nm) in band 1 and $\Delta\nu_{2,3} \approx 0.26\,cm^{-1}$ ($\Delta\lambda_2 \approx 0.07$ and $\Delta\lambda_3 \approx 0.1$ nm) in bands 2 and 3. In order to improve the dynamic range of the instrument, the scientific measurements of TANSO-FTS are performed in two gain modes, medium (M) and high (H), used according to the measured level of intensity. For example, gain M is used over bright surfaces such as deserts. With an instantaneous field of view (IFOV) of 15.8 mrad (~ 10.5 km diameter at nadir when projected to the ground), TANSO-FTS can measure $\pm 35°$ across track and $\pm 20°$ along track. The typically used scan time of one interferogram is 4 s. Between 4 April 2009 and 31 July 2010, the five-point across track mode was used, which yields footprints separated by ~ 158 km across track and ~ 152 km along track at the equator (e.g. Crisp et al., 2012). In order to improve the pointing stability during the scans, on 1 August 2010 the observation mode was changed to a three-point across track mode with footprints separated by ~ 263 km across track and ~ 283 km along track at the equator.

The TANSO-CAI instrument is a high spatial resolution imager detecting clouds and optically thick aerosol layers within the TANSO-FTS field of view. The TANSO-CAI data products are not used for the BESD algorithm.

4 SCIAMACHY BESD algorithm

The BESD retrieval algorithm has been developed at the University of Bremen to retrieve XCO_2 from SCIAMACHY nadir measurements. BESD aims to minimise scattering-related errors of the retrieved XCO_2. For this purpose, the algorithm explicitly accounts for scattering. The theoretical basis of BESD and a study of synthetic retrievals is presented in the publication of Reuter et al. (2010) and validation results are presented in Reuter et al. (2011).

The algorithm is a core algorithm within ESA's CCI (Hollmann et al., 2013; Buchwitz et al., 2013b; Dils et al., 2014) aiming at delivering high-quality satellite retrievals. Here we use the most recent product version (02.00.08) of SCIAMACHY BESD, which is part of the Climate Research Data Package (CRDP#2) of the CCI project. A detailed description of the current version of BESD can be found in the Algorithm Theoretical Basis Document (ATBD) (Reuter et al., 2014a, available at http://www.esa-ghg-cci.org/). Here, only a short overview of the algorithm is given.

The BESD algorithm retrieves several independent parameters from the O_2-A band (755–775 nm) in SCIAMACHY's channel 4 and from a CO_2 band (1558–1594 nm) in channel 6. An optimal-estimation-based inversion technique is used to derive the most probable atmospheric state from

a SCIAMACHY measurement using some a priori knowledge. The state vector consists of 26 elements. These elements include a wavelength shift and the full width half maximum (FWHM) of a Gaussian-shaped instrumental slit function, both fitted separately in the O_2 and CO_2 fit window. A Lambertian surface albedo with smooth spectral progression expressed as a second-order polynomial (with polynomial coefficients P_0, P_1 and P_2) is fitted separately in both fit windows. A 10-layered CO_2 mixing ratio profile, which is separated in equally spaced pressure intervals, is fitted in the CO_2 fit window. The correlated a priori errors of the CO_2 profile layers provide a degree of freedom of the retrieved XCO_2 of ~ 1.0. Reanalysis profiles (ERA-Interim, Dee et al., 2011) of pressure, temperature and humidity provided by the ECMWF are used for the forward model calculation needed to calculate simulated SCIAMACHY spectra. The surface pressure, a shift of the temperature profile and the H_2O column-averaged mole fraction are fitted in the O_2 and CO_2 window simultaneously.

Atmospheric scattering is considered by fitting three scattering-related parameters. A thin ice cloud layer consisting of fractal ice crystals with 50 µm effective radius and a thickness of 0.5 km is defined for the forward model calculations. Within the retrieval, the cloud water path (CWP) and the cloud top height (CTH) are retrieved. Aerosols are considered by using a standard LOWTRAN summer aerosol profile with moderate rural aerosol load. A Henyey–Greenstein phase function is used and the total optical thickness is about 0.136 at 750 nm and 0.038 at 1550 nm. The aerosol retrieval is based on scaling the predefined aerosol profile (aerosol profile scaling (APS) factor). Not only the scattering parameters but also the parameters defining the meteorological situation are fitted simultaneously via a merged fit window approach. Simultaneous fitting in both fit windows transfers information, e.g. in case of scattering parameters, mostly obtained from the O_2-A band to the CO_2 band.

The forward model is the radiative transfer model SCIATRAN (Rozanov et al., 2014). SCIATRAN calculates the needed radiance spectra and weighting functions, which are the derivatives of the measured radiation. The correlated-k approach of Buchwitz et al. (2000) is used to accelerate the radiative transfer calculations. Line parameters from NASA's absorption cross section database ABSCO v4.0 (Thompson et al., 2012) is used for O_2. The HITRAN 2008 database (Rothman et al., 2009) are used for the other gases. The calculated spectra are convolved with a Gaussian slit function.

Although BESD has been designed to minimise scattering-related retrieval errors, clouds are still an important potential error source and strict cloud filtering is necessary. BESD filters clouds by using cloud information based on measurements of the Medium Resolution Imaging Spectrometer (MERIS).

The post-processing of the retrieved data includes strict quality filtering and an empirical bias correction. This is needed due to the demanding accuracy requirements on the satellite retrievals. The implemented bias correction for SCIAMACHY BESD is described in the BESD ATBD (Reuter et al., 2014a).

5 GOSAT BESD algorithm

The GOSAT BESD algorithm is based on the SCIAMACHY BESD algorithm which has been modified to also retrieve XCO_2 from GOSAT. Here, an overview of the modifications of BESD are given.

5.1 Level 1C data generation

GOSAT BESD uses GOSAT Level 1B data (L1B) version 161160. These data have been obtained from the GOSAT User Interface Gateway (http://data.gosat.nies.go.jp/GosatUserInterfaceGateway/guig/GuigPage/open.do) and from ESA's GOSAT Third Party Mission data archive. The (uncalibrated) L1B data have been converted into calibrated Level 1C (L1C) data, by using e.g. the radiance correction scheme described by Yoshida et al. (2012). The L1C data consist of the fully calibrated total intensity, an estimation of the measurement error and a priori information. The total intensity is computed by using the polarisation synthesis method described by Yoshida et al. (2011) using the Mueller matrices described by Kuze et al. (2009). The measurement noise ($\varepsilon_{\text{meas}}$) is estimated by the standard deviation of the first 500 and the last 500 off-band spectral points of GOSAT bands 1, 2 and 3. These spectral points lie outside the band pass filter and can therefore provide a good estimate of $\varepsilon_{\text{meas}}$. However, using only the estimate of the measurement noise for the retrieval neglects the contribution of the forward model error. Therefore, empirical noise ($\varepsilon_{\text{empirical}}$) has been implemented and used as described by Yoshida et al. (2013) and Crisp et al. (2012). In order to account for the forward model error, we make the same assumptions as done by Yoshida et al. (2013). We assume that our forward model error increases as the signal-to-noise ratio (SNR) increases. Using the same formula as given by Yoshida et al. (2013),

$$\varepsilon_{\text{empirical}} = \varepsilon_{\text{meas}} \cdot \sqrt{a_0 + a_1 \text{SNR} + a_2 \text{SNR}^2}, \quad (1)$$

and evaluating the relationship between SNR and the mean squared values of the residual spectra delivers the coefficients a_0, a_1 and a_2 in each spectral window. The coefficients are listed in Table 1.

The a priori information includes profiles of temperature, pressure and humidity obtained from ECMWF data and height information from a digital elevation model (DEM). The used DEM (obtained from http://www.viewfinderpanoramas.org) is mostly based on data collected in 2000 by the Shuttle Radar Topography Mission and has a spatial resolution of 15 arc s. A priori estimates for the zeroth-order polynomial coefficient of the albedo (P_0) are obtained by computing the 95 % percentile of the reflectance

Table 1. Coefficients for empirical noise for GOSAT high (H) and medium (M) gain observations over land.

Gain mode	Emp. noise coef.	Band 1 (O_2 A) (12 920–13 195 cm^{-1})	Band 2 (weak CO_2) (6170–6278 cm^{-1})	Band 3 (strong CO_2) (4804–4896 cm^{-1})
H	a_0	1.157	1.285	1.217
	a_1	-1.843×10^{-3}	-1.639×10^{-3}	-2.301×10^{-3}
	a_2	1.506×10^{-5}	8.073×10^{-6}	2.755×10^{-5}
M	a_0	1.256	1.091	0.6401
	a_1	-2.010×10^{-3}	-7.783×10^{-3}	1.957×10^{-3}
	a_2	1.430×10^{-5}	6.615×10^{-6}	2.346×10^{-5}

(sun-normalised GOSAT intensity divided by the cosine of the solar zenith angle).

5.2 GOSAT XCO_2 (Level 2) generation

The GOSAT XCO_2 (Level 2) data have been generated by using a modified version of the SCIAMACHY BESD retrieval algorithm. The main modifications are the following: we have used three bands instead of two bands (as used for SCIAMACHY) for the retrieval of GOSAT XCO_2. Band 1 includes the O_2-A band (12 920–13 195 cm^{-1} or 758–774 nm), band 2 contains a weak CO_2 absorption band (6170–6278 cm^{-1} or 1593–1621 nm) and band 3 includes a strong CO_2 absorption band (4804–4896 cm^{-1} or 2042–2082 nm).

The state vector of GOSAT BESD consists of 38 elements instead of 26 for SCIAMACHY BESD. The state vector elements, their a priori values and uncertainties are listed in Table 2. A second-order albedo polynomial is additionally fitted in the third fit window. Besides a spectral shift of the nadir radiance, a shift of the solar spectrum is fitted. Instead of the FWHM of a SCIAMACHY Gaussian slit function, parameters defining the instrumental line shape function (ILS) of TANSO-FTS are fitted. These parameters are the maximum optical path difference (MOPD) and the IFOV. The ILS is calculated (similar as done by e.g. Reuter et al., 2012a) from

$$\mathrm{ILS}(\nu) \propto \Pi\left(\frac{8\nu}{\nu_0 \mathrm{IFOV}}\right) \otimes \mathrm{sinc}(2\nu \cdot \mathrm{MOPD}). \quad (2)$$

Here, ν is the wavenumber (centred around 0), Π is a boxcar function, the $\otimes$ is the convolution operator and ν_0 is the centre wavenumber.

A temperature shift, the column-averaged mole fraction of water vapour and the surface pressure are fitted as for SCIAMACHY BESD and also the CO_2 profile consists of 10 layers. The CO_2 a priori profile is obtained by using the Simple Empirical CO_2 Model (SECM) described by Reuter et al. (2012b). The a priori uncertainty of the CO_2 profile has been scaled (similar to Reuter et al., 2010) so that the a priori XCO_2 uncertainty is about 42 ppm. This large value enables that the XCO_2 retrieval is virtually unconstrained.

Contributions from plant fluorescence and the impact of a non-linearity response of the incident radiation to the intensity in the mostly affected band 1 can be reduced by fitting a wavenumber independent offset (also called zero-level offset) (Butz et al., 2011). This has also been implemented in GOSAT BESD for the O_2-A band.

The fit parameters defining atmospheric scattering are the same as for SCIAMACHY BESD, namely CWP, CTH and APS. The defined thin cloud layer consists of fractal ice particles with an effective radius of 100 µm.

The much higher spectral resolution of GOSAT is the reason why the radiative transfer model SCIATRAN cannot run in the implemented computational efficient correlated-k mode used for SCIAMACHY BESD. However, in order to accelerate the radiative transfer calculations for GOSAT BESD retrievals, tabulated cross sections (based on the absorption cross sections database ABSCO v4.0 described by Thompson et al., 2012) have been used and the linear-k scheme of Hilker (2015) has been implemented. A high spectral resolution solar irradiance spectrum based on the "OCO TOON spectrum" (O'Dell et al., 2012) is used to calculate the total intensity instead of the sun-normalised intensity as used by SCIAMACHY BESD. The simulated intensity is convolved with the GOSAT ILS (Eq. 2).

In Fig. 1 a typical example of observed and fitted GOSAT spectra in all three fitting windows is presented. The observed and fitted spectra show reasonable agreement. The reduced χ^2 (computed as described by Yoshida et al., 2013) is in all three fitting windows ~ 1, which means that the difference between observed and fitted spectra agrees with the estimated noise.

5.3 Cloud filtering and post-processing

Even thin clouds are a main error source for satellite XCO_2 retrievals. Therefore, GOSAT BESD includes a cloud detection method similar to Yoshida et al. (2011) and Heymann et al. (2012b). The intensity from a saturated water vapour absorption band at 1.9 µm is used and clouds are detected by using a threshold technique. The basic idea behind this method is that in the clear-sky case, the amount of radiation measured by GOSAT is very small as essentially all

Table 2. State vector elements of the GOSAT BESD retrieval algorithm.

State vector element	Quantities	A priori value	A priori uncertainty
Albedo 0th polynomial coef. (P_0)	3	estimated from computed reflectance	0.1
Albedo 1st polynomial coef. (P_1)	3	0.0	0.01
Albedo 2nd polynomial coef. (P_2)	3	0.0	0.001
Spectral shift	3	estimated from the position of Fraunhofer lines	0.1 cm^{-1}
Shift of the solar spectrum	3	estimated from the position of Fraunhofer lines	0.1 cm^{-1}
Maximum optical path difference	3	2.5 cm	0.05 cm
Instantaneous field of view	3	15.8 mrad	0.005 mrad
Zero-level offset	1	0.0 (in units 10^9 W cm^{-2} cm sr^{-1})	1.0
CO_2 profile	10	based on SECM CO_2 model	see Reuter et al. (2010)
Surface pressure	1	based on ECMWF data	5 hPa
Temperature scaling	1	based on ECMWF data	see Reuter et al. (2010)
Water vapour profile scaling	1	based on ECMWF data	see Reuter et al. (2010)
Cloud water path	1	1 g m^{-2}	1 g m^{-2}
Cloud top height	1	10 km	2 km
Aerosol profile scaling	1	1.0	0.2

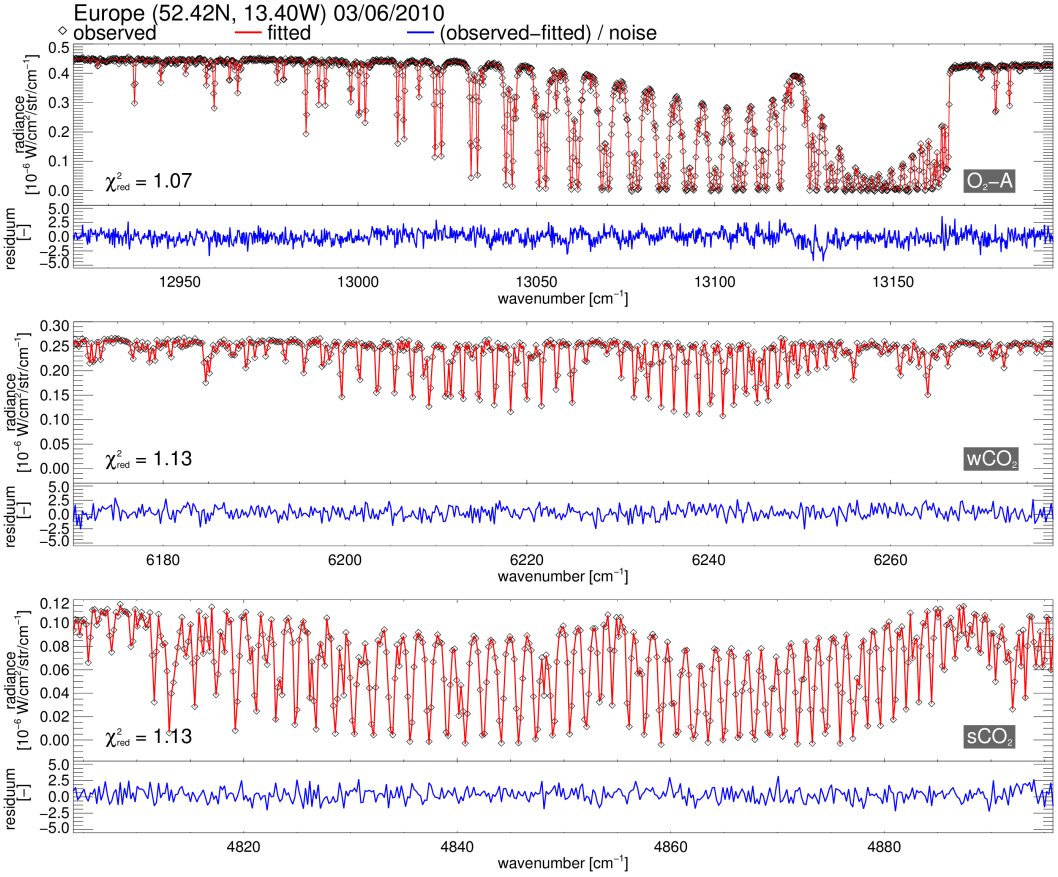

Figure 1. Observed (black) and fitted (red) intensity (radiance) and its residuum (blue) over a typical scene in Germany, near Berlin (52.42° N, 13.40° E) on 3 June 2010. Top panel: observed and fitted radiance and the residuum for GOSAT band 1 (12 920–13 195 cm^{-1}). Middle panel: as top panel but for band 2 (6170–6278 cm^{-1}). Bottom panel: as top panel but for band 3 (4804–4896 cm^{-1}).

Table 3. Parameters and thresholds as used for the quality filtering. A scene is considered to be of "good" quality if e.g. the albedo difference between the fitted and a priori albedo in band 2 (albedo difference, weak CO_2) is larger than the lower threshold of -0.02 and smaller than the upper threshold of 0.02.

Parameter	Lower threshold	Upper threshold
Number of iterations	–	16
Albedo difference (weak CO_2)	-0.02	0.02
Albedo second polynomial coef. (weak CO_2)	–	0.0003
Albedo slope (strong CO_2)	–	-0.003
Albedo second polynomial coef. (strong CO_2)	-0.0005	–
χ^2 (O_2-A)	–	1.2
χ^2 (weak CO_2)	–	2.0
χ^2 (strong CO_2)	–	2.2
RMSE (weak CO_2)	–	0.007
Error reduction	0.92	–
XCO_2 uncertainty	–	2.6 ppm
IFOV (O_2-A)	15.35 mrad	15.9 mrad
IFOV (weak CO_2)	15.5 mrad	–
Surface pressure difference	-30 hPa	20 hPa
Air-mass factor	–	3.5
Viewing zenith angle	–	40°

photons are absorbed by tropospheric water vapour. When a cirrus cloud is located above most of the atmospheric water vapour, a significant amount of radiation can be backscattered and measured. A cloud is detected when the measured intensity is larger than a threshold. We use 4 times the measurement noise as threshold, which has been empirically determined. This filter is sensitive to high ice clouds but not that sensitive to low water clouds. Therefore, we also filter for bright scenes by using the a priori P_0 (zeroth-order polynomial coefficient of the albedo) obtained from GOSAT reflectances (see Sect. 5.1). If the a priori P_0 is larger than a threshold, the measurement is considered to be cloud contaminated. The threshold for this filter is 0.7 and has also been empirically determined. In addition to these cloud filters, the quality filtering removes still remaining potentially cloud-contaminated scenes.

The high demands on the satellite retrievals require strict quality filtering not only for clouds. In order to minimise biases and to reduce the scatter of the data, GOSAT BESD uses filter thresholds for selected parameters. The used parameters and their filter thresholds have been selected by evaluating GOSAT XCO_2 biases and are shown in Table 3. These parameters include e.g. parameters defining the quality of the spectral fit (χ^2, RMSE), scattering parameters (CWP, APS) and parameters defining the meteorological state (difference between fitted and a priori surface pressure).

Systematic errors have been additionally reduced by using a global bias correction scheme (similar as done by Schneising et al., 2013; Wunch et al., 2011b; Guerlet et al., 2013). We use TCCON data from all stations listed in Table 4 for the evaluation of the coefficients of the bias correction. As TCCON is used here as reference, the differences to TCCON can be interpreted as the systematic retrieval errors. Figure 2 shows the dependence of the non-bias-corrected GOSAT BESD–TCCON XCO_2 differences on the four most relevant retrieval parameters. The four parameters are the viewing zenith angle (VZA), the air-mass factor (AMF), P_0 of band 1 (ALB) and the difference to the a priori P_0 of band 2 (ALBDIFF). These parameters show a linear or quadratic dependence on these differences.

Table 4. Used TCCON sites, their location, altitude (above sea level) and used observation period.

Station	Latitude [°]	Longitude [°]	Altitude [km]	Used observation period
Sodankylä	67.37	26.63	0.188	12/02/2009–26/02/2013
Białystok	53.23	23.03	0.180	01/03/2009–30/04/2013
Bremen	53.10	8.85	0.270	24/03/2005–07/05/2013
Karlsruhe	49.10	8.44	0.120	19/04/2010–28/05/2013
Orleans	47.97	2.11	0.130	29/08/2009–07/03/2013
Garmisch	47.49	11.06	0.740	16/07/2007–28/05/2013
Park Falls	45.95	-90.27	0.440	02/06/2004–07/12/2013
Four Corners	36.80	-108.48	1.643	10/03/2011–30/05/2013
Lamont	36.60	-97.49	0.320	06/07/2008–31/12/2013
Tsukuba	36.05	140.12	0.030	25/12/2008–11/01/2013
JPL	34.20	-118.18	0.390	01/07/2007–31/03/2013
Saga	33.24	130.29	0.007	28/07/2011–26/05/2013
Izaña	28.30	-16.50	2.370	18/05/2007–23/02/2013
Darwin	-12.42	130.89	0.030	01/09/2005–30/05/2013
Wollongong	-34.41	150.88	0.030	26/06/2008–30/05/2013
Lauder	-45.04	169.68	0.370	29/06/2004–01/12/2013

To reduce the systematic errors in the GOSAT BESD XCO_2 data set, the following equation has been used:

$$\mathrm{XCO_2^{cor}} = \mathrm{XCO_2} + b_0 + b_1 \cdot \mathrm{ALBDIFF} + b_2 \cdot \mathrm{VZA} + b_3 \cdot \mathrm{VZA}^2 + b_4 \cdot \mathrm{AMF} + b_5 \cdot \mathrm{AMF}^2 + b_6 \cdot \mathrm{ALB}. \quad (3)$$

The coefficients found by multivariate linear regression are $b_0 = 0.4490$ ppm, $b_1 = 236.8$ ppm, $b_2 = -0.1096$ ppm $(°)^{-1}$, $b_3 = 6.750 \times 10^{-3}$ ppm $(°)^{-2}$, $b_4 = 5.961$ ppm, $b_5 = -1.912$ ppm and $b_6 = -8.212$ ppm. After application of the bias correction the dependence on the four parameters is significantly reduced (see right panels

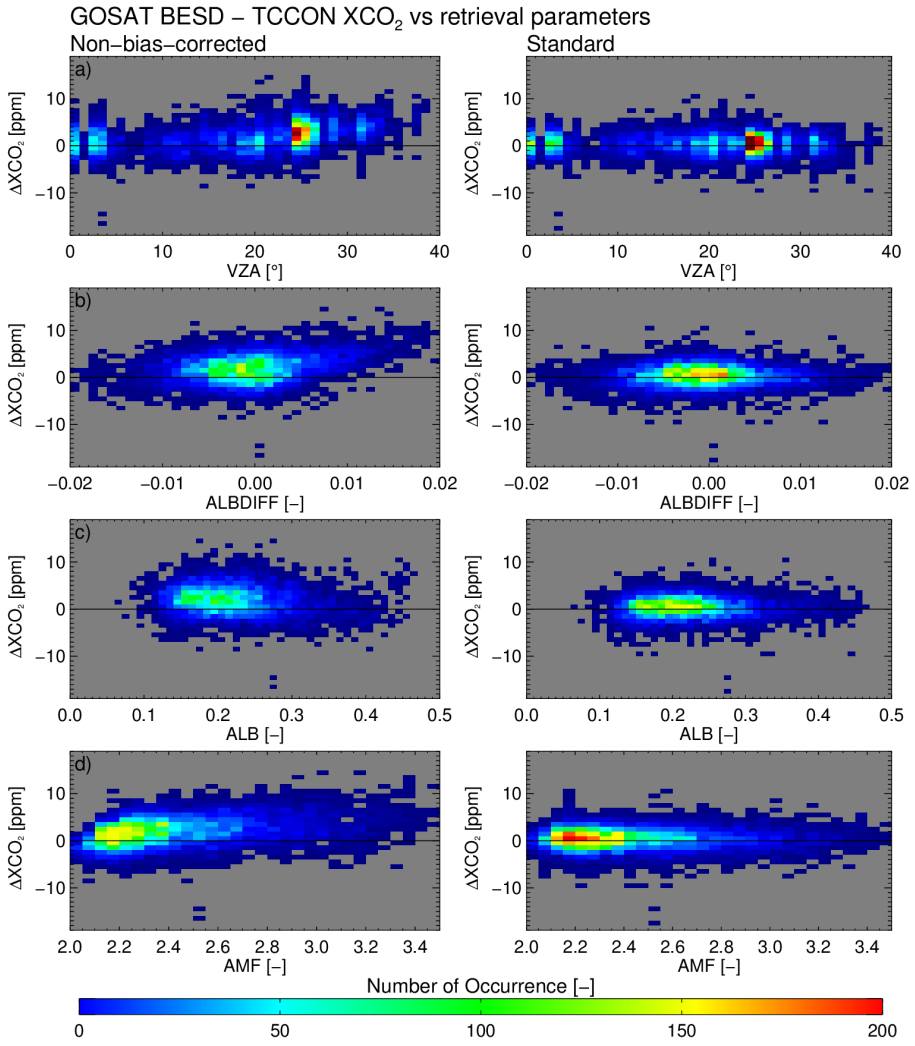

Figure 2. Two-dimensional histograms of non-bias-corrected (left) and standard (bias-corrected, right) GOSAT BESD–TCCON XCO_2 differences versus the following four retrieval parameters: **(a)** viewing zenith angle (VZA), **(b)** difference of retrieved to a priori albedo P_0 of band 2 (ALBDIFF), **(c)** retrieved P_0 of band 1 (ALB) and **(d)** air-mass factor (AMF).

of Fig. 2). Our standard product is the bias corrected GOSAT BESD XCO_2 data set and the version used here is 01.00.02.

6 Intercomparisons between TCCON, SCIAMACHY and GOSAT XCO_2

The quality of the satellite XCO_2 data products and their consistency has been assessed using ground-based TCCON XCO_2 observations. In this section a short overview of TCCON is given, the assessment method is described and the comparison results are discussed.

6.1 TCCON observations

The Total Carbon Column Observing Network (TCCON) (Wunch et al., 2011a) consists of several ground-based measurement stations of Fourier transform spectrometers (FTS). The FTS instruments measure the absorption of direct sunlight by gases. This has the advantage of being less influenced by atmospheric scattering compared to satellite measurements. From the measured spectra TCCON retrieves XCO_2, i.e. the same quantity as retrieved from satellite instruments. TCCON achieves a precision and accuracy of 0.4 ppm (1σ) (Wunch et al., 2010; Messerschmidt et al., 2011). In this study, we use TCCON version GGG2012 considering all recommended corrections from http://tccon-wiki.caltech.edu. For a comprehensive validation, data from as many TCCON stations as possible need to be used. Therefore, we have used 16 TCCON stations for the

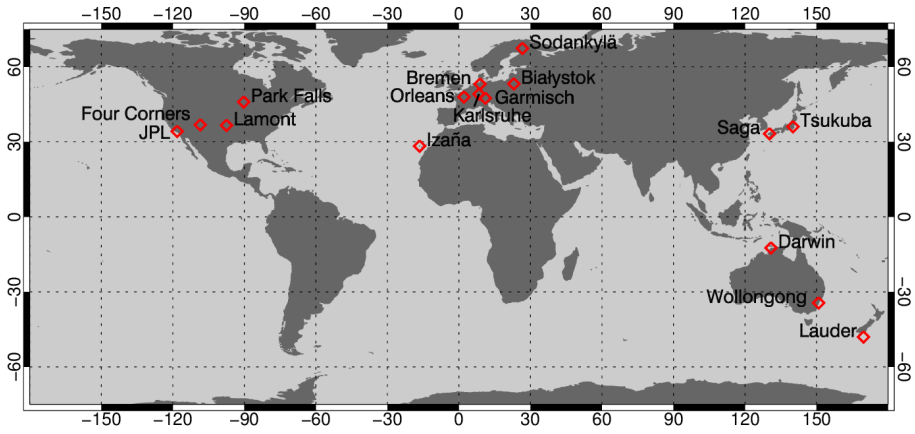

Figure 3. TCCON stations used for validation.

validation that have an overlapping observation period with SCIAMACHY and GOSAT. The used stations are shown in Fig. 3 and listed in Table 4.

6.2 Method

The first part of this study is the validation of the GOSAT BESD (available for January 2010–December 2013) and SCIAMACHY BESD XCO_2 (available for August 2003–March 2012) data sets using TCCON XCO_2. In order to evaluate the consistency of the satellite data products, we compare the data products with TCCON data for the same time period and perform a direct comparison of the satellite data, i.e. validation results from the overlapping observation years 2010–2011 of SCIAMACHY and GOSAT are presented and compared, and a direct comparison of daily means of the data sets and an additional comparison to daily TCCON data are performed.

The comparison between different CO_2 data sets from measurements of different instruments is not trivial because of the different averaging kernels and a priori information as used by the different retrieval algorithms. To ensure that the differences between the measurements are not dominated by differences of the averaging kernels and a priori information, Rodgers (2000) recommends adjusting the measurements by using a common a priori profile and accounting for the averaging kernels. As SCIAMACHY BESD and GOSAT BESD already use the same a priori profiles obtained from the SECM model (Reuter et al., 2012b), only the TCCON measurements need to be adjusted. However, for TCCON, the CO_2 averaging kernels are typically very close to unity and the used a priori profiles only marginally differ from the SECM profiles as SECM is based on CarbonTracker CO_2 (Peters et al., 2007), which is similar to the TCCON a priori. Reuter et al. (2011) found that adjusting the FTS measurements results in only small modifications of about 0.1 ppm. This is small compared to the precision of SCIAMACHY and GOSAT retrievals. Therefore, the FTS measurements are not adjusted.

All TCCON measurements 2 hours before or after the satellite measurement and all satellite data within a $10° \times 10°$ box surrounding the TCCON stations are used. We have also tested other collocation criteria such as a 5° and a 350 km radius around the TCCON sites. The results of the intercomparison of the data sets using these collocation criteria have been similar to the $10° \times 10°$ box (see Table S1, S2 and S3 in the Supplement). For the results presented here we have decided to use the $10° \times 10°$ box collocation criterion as it provided the largest amount of collocated data points.

Four values have been obtained from the comparisons of the data sets at the TCCON sites: (i) the number of collocated data points, (ii) the mean difference between the data sets (can be interpreted as a regional bias), (iii) the standard deviation of the difference (is an estimate of the precision when compared with TCCON) and (iv) the linear correlation coefficient between the data sets.

6.3 Results

6.3.1 Entire time series

Figure 4 shows time series of BESD and TCCON XCO_2 at the Lamont and Darwin TCCON sites. The qualitative comparison between SCIAMACHY BESD and GOSAT BESD XCO_2 indicates good consistency between the data sets as the satellite data are in reasonable to good agreement among themselves and with TCCON. This has been further investigated by more quantitative comparisons.

In Fig. 5a all collocated GOSAT and TCCON XCO_2 data between 2010 and 2013 and Fig. 5b all collocated SCIAMACHY and TCCON XCO_2 data between 2002 and 2012 are presented. The number of collocations are higher for SCIAMACHY/TCCON compared to GOSAT/TCCON as the time series of BESD SCIAMACHY is longer and more measurements per day were performed by SCIA-

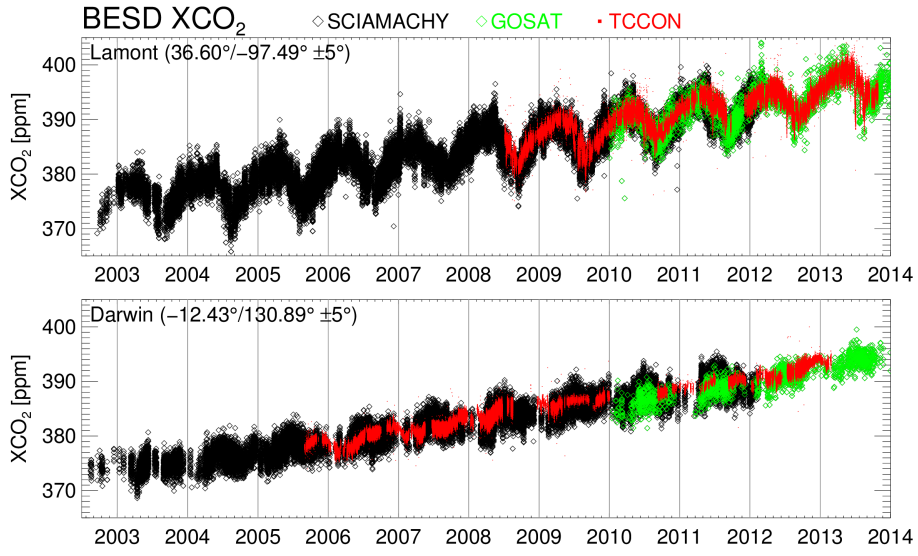

Figure 4. SCIAMACHY BESD (black), GOSAT BESD (green) and TCCON (red) XCO_2 at the Lamont (top) and Darwin (bottom) TCCON sites (± 2 h, $10° \times 10°$).

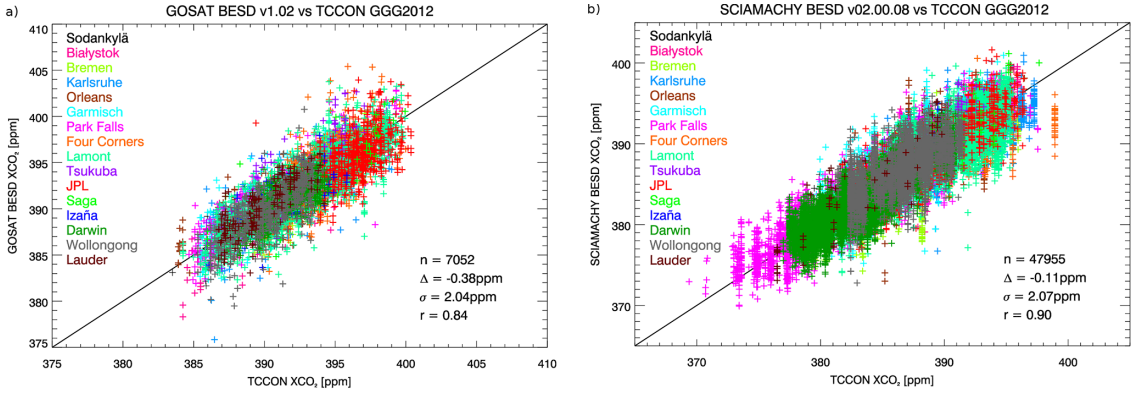

Figure 5. Scatter plots of individual satellite vs. TCCON XCO_2 measurements at the chosen TCCON sites. **(a)** GOSAT BESD XCO_2 (January 2012–December 2013) vs. TCCON XCO_2. **(b)** SCIAMACHY BESD XCO_2 (August 2002–March 2012) vs. TCCON XCO_2. n is the number of collocations, Δ is the mean difference between the satellite-based data and TCCON, σ is the standard deviation of the difference and r is the correlation coefficient.

MACHY. The mean difference to TCCON is -0.38 ppm for GOSAT and -0.11 ppm for SCIAMACHY. The standard deviation of the difference to TCCON is similar ($\sim$ 2 ppm) for GOSAT and SCIAMACHY. The correlation coefficient between GOSAT/TCCON is 0.84 and between SCIAMACHY/TCCON 0.90.

In more detail, the comparison results between GOSAT BESD XCO_2 and TCCON are shown in Table 5 (full time series, standard). The standard deviation of the difference is between 1.36 ppm (Darwin) and 2.65 ppm (Karlsruhe); the station bias to TCCON is in the range -0.92 ppm (JPL) to 2.07 ppm (Tsukuba) and the correlation coefficient between GOSAT BESD and TCCON is between 0.57 (JPL) and 0.89 (Park Falls). The comparison results at the Izaña TCCON site should be interpreted with care as some of the collocated GOSAT data could be measured over scenes with a large altitude difference to the Izaña site (altitude of 2.37 km). Also shown are the results for the non-bias-corrected GOSAT BESD XCO_2. Due to the found systematic retrieval errors, the station biases are between -3.56 ppm (Sodankylä) and 1.37 ppm (Tsukuba), the standard deviation of the difference is between 3.35 ppm (Karlsruhe) and 1.94 ppm (Darwin) and the correlation coefficient is between 0.44 (JPL) and 0.82 (Park Falls, Tsukuba).

Table 6 shows the detailed results of the comparison between the SCIAMACHY BESD XCO_2 data and the TCCON measurements for the full SCIAMACHY BESD data set (ranging from mid-2002 to mid-2012). The standard deviation of the difference is between 1.72 ppm (Darwin) and 3.03 ppm (Lauder). The station biases are between

Table 5. Results of the comparison between GOSAT BESD and TCCON XCO_2 for individual (single measurement) satellite data. Shown are the results for non-bias corrected and standard (bias-corrected) GOSAT BESD of the full time series (January 2010–December 2013, see Fig. S1 for the time series of the standard GOSAT BESD) of the data set and for a 2010–2011 sub-set of the standard GOSAT BESD data product. Δ is the mean difference between GOSAT BESD and TCCON XCO_2, σ is the standard deviation of the difference, r is the correlation coefficient between the time series and n the number of collocations. Stations marked with * have less than 30 collocations in one of the comparisons of GOSAT BESD or SCIAMACHY BESD XCO_2 with TCCON XCO_2. Therefore, these comparisons should be interpreted with care. The mean offset (mean of the mean differences), the estimated single measurement precision (mean of the standard deviation of the difference), the mean correlation coefficient and the station-to-station bias (standard deviation of the mean differences) are calculated without these stations.

Station	Full data set							2010–2011			
	Non-bias-corrected			Standard				Standard			
	Δ [ppm]	σ [ppm]	r [–]	Δ [ppm]	σ [ppm]	r [–]	n [–]	Δ [ppm]	σ [ppm]	r [–]	n [–]
Sodankylä	−3.56	2.58	0.71	−0.16	1.97	0.79	37	−0.17	1.93	0.78	32
Białystok	−2.41	3.00	0.78	−0.53	2.15	0.88	185	−0.75	2.26	0.78	97
Bremen	−1.39	2.38	0.77	−0.88	2.31	0.76	54	−1.01	2.25	0.65	45
Karlsruhe	−1.53	3.35	0.64	−0.65	2.65	0.76	271	−0.58	2.67	0.69	173
Orleans	−0.98	2.90	0.54	−0.04	2.21	0.69	140	−0.12	2.24	0.66	121
Garmisch	−0.47	3.21	0.66	0.60	2.50	0.78	239	0.52	2.30	0.72	159
Park Falls	−0.83	2.61	0.82	0.25	1.96	0.89	402	0.19	1.79	0.79	193
Four Corners	−1.83	2.66	0.72	−0.36	2.12	0.78	1145	−0.77	2.14	0.68	375
Lamont	−2.05	2.51	0.78	−0.48	1.91	0.86	2199	−0.47	1.88	0.77	959
Tsukuba*	1.37	2.63	0.82	2.07	2.41	0.85	83	1.16	1.94	0.64	14
JPL*	−2.65	3.15	0.44	−0.92	2.06	0.57	656	−1.95	2.02	−0.48	14
Saga*	−1.87	3.30	0.80	0.03	2.26	0.88	43	−0.02	2.52	0.37	20
Izaña*	−1.36	2.31	0.63	−0.33	2.09	0.64	68	−0.01	2.13	0.52	43
Darwin	−2.42	1.94	0.60	−0.64	1.36	0.73	655	−1.00	1.24	0.59	163
Wollongong	−2.89	2.91	0.66	−0.43	1.84	0.76	736	−0.43	1.76	0.65	340
Lauder*	−0.18	3.07	0.62	0.46	1.72	0.80	139	0.33	1.84	0.33	50
MEAN	−1.85	2.78	0.69	−0.30	2.09	0.79		−0.42	2.04	0.71	
SD	0.93			0.43				0.48			

Table 6. As Table 5 but for SCIAMACHY BESD XCO_2 full data set (August 2003–March 2012, see Fig. S2 for the time series) and for a 2010–2011 sub-set.

Station	Full data set				2010–2011			
	Δ [ppm]	σ [ppm]	r [–]	n [–]	Δ [ppm]	σ [ppm]	r [–]	n [–]
Sodankylä	1.11	1.97	0.89	271	1.10	1.77	0.89	171
Białystok	0.23	2.29	0.77	1689	0.13	2.67	0.62	763
Bremen	−0.85	2.37	0.87	1788	−1.07	1.68	0.86	667
Karlsruhe	−0.61	2.52	0.70	1869	−0.51	2.55	0.65	1728
Orleans	0.26	2.48	0.78	1334	0.42	2.55	0.45	942
Garmisch	1.20	2.43	0.85	1987	0.98	2.51	0.59	906
Park Falls	0.30	2.07	0.93	5375	0.75	1.92	0.71	1663
Four Corners	−1.95	2.35	0.38	637	−1.61	2.10	0.37	523
Lamont	−0.19	1.89	0.85	16 520	−0.37	1.91	0.67	7204
Tsukuba*	2.36	2.35	0.74	62	2.57	2.20	0.37	23
JPL*	−0.46	2.29	0.88	1016	−0.05	2.02	0.22	64
Saga*	0.06	2.63	0.55	60	−0.32	2.38	0.16	55
Izaña*	1.75	2.12	0.81	11	2.66	2.43	0.92	6
Darwin	−0.35	1.72	0.85	11 044	−0.87	1.67	0.64	730
Wollongong	0.25	2.09	0.69	4233	0.13	2.04	0.45	2535
Lauder*	1.11	3.03	0.90	59	1.31	3.44	0.74	11
MEAN	−0.05	2.20	0.78		−0.08	2.12	0.63	
SD	0.89				0.88			

−1.95 ppm (Four Corners) and 2.36 ppm (Tsukuba). The correlation coefficient is typically high and is between 0.38 (Four Corners) and 0.93 (Park Falls). The low correlation coefficient at Four Corners can be explained by the dependence of the correlation coefficient on the length of the time series. At Four Corners SCIAMACHY and TCCON have collocations only in 1 year compared to 8 years at Park Falls. An additional explanation for the low correlation at Four Corners can be the collocation criterion. There are two large power plants in the vicinity of the Four Corners TCCON station introducing large variability (Lindenmaier et al., 2014) which can be smeared out in the satellite data by using the $10^\circ \times 10^\circ$ collocation criterion. This may also be a reason for the large −1.95 ppm mean difference to TCCON at Four Corners.

In order to summarise the results, we calculate the mean standard deviation of the difference (can be interpreted as an upper limit for the single measurement precision) and the standard deviation of the station biases, which we interpret as the station-to-station bias deviation (short: station-to-station bias). For the sake of completeness, we also calculate the mean of the station biases (mean offset) and the mean correlation coefficient. However, the mean offset is less relevant as it can be easily adjusted. In order to determine robust values, we have excluded TCCON stations with less than 30 measurements in one of the comparisons, i.e. Tsukuba, JPL, Saga, Izaña and Lauder are not considered.

The full data set analysis (GOSAT: January 2010–December 2013; SCIAMACHY: August 2002–March 2012) shows for the standard GOSAT BESD data set a mean offset of −0.30 ppm, a single measurement precision of 2.09 ppm, a mean correlation coefficient of 0.79 and a station-to-station bias of 0.43 ppm. Compared to the non-bias-corrected GOSAT BESD data set (mean offset of −1.85 ppm, single measurement precision of 2.78 ppm, mean correlation coefficient of 0.69 and station-to-station bias of 0.93 ppm) the quality of the standard (bias-corrected) GOSAT BESD data set is enhanced as the implemented bias correction scheme reduces systematic retrieval errors. The results for the standard GOSAT BESD data set are similar to results of other XCO_2 products from retrieval algorithms applied to GOSAT observations; e.g. Dils et al. (2014) found for the full-physics algorithm of the University of Leicester (Cogan et al., 2012) a mean offset of −0.76 ppm, a single measurement precision of 2.37 ppm, a mean correlation coefficient of 0.79 and a station-to-station bias of 0.53 ppm and for SRON's RemoTeC algorithm (Butz et al., 2011) a mean offset of −0.57 ppm, a mean single measurement precision of 2.50 ppm, a mean correlation coefficient of 0.81 and a station-to-station bias of 0.75 ppm. Note that both data sets are bias corrected as well. They used GOSAT data between April 2009 and April 2011, a collocation time of ± 2 h and all measurements within a 500 km radius around a TCCON site.

The SCIAMACHY BESD data have a mean offset of −0.05 ppm, a single measurement precision of 2.20 ppm, a mean correlation coefficient of 0.78 and a station-to-station bias of 0.89 ppm. The mean offset, the mean single measurement precision and the mean correlation coefficient are similar to the findings of Dils et al. (2014). They found a mean offset of 0.02 ppm, a slightly larger single measurement precision of 2.53 ppm and a mean correlation of 0.81. The station-to-station bias found by Dils et al. (2014) is slightly better with 0.63 ppm. A reason for this difference is the large mean difference from TCCON at Four Corners (−1.95 ppm). Without Four Corners the mean offset (0.14 ppm), the mean correlation coefficient (0.82) and the mean single measurement precision (2.18 ppm) remain nearly the same, but the station-to-station bias (0.67 ppm) becomes better and similar to the findings of Dils et al. (2014).

6.3.2 Overlapping time series (2010–2011)

For the comparison of the validation results of GOSAT BESD and SCIAMACHY BESD, we have used the time period 2010 to 2011 where both data sets overlap. Both data sets have a negative station bias e.g. at Bremen (−1.01 ppm for GOSAT and −1.07 ppm for SCIAMACHY), Darwin (−1.00 ppm for GOSAT and −0.87 ppm for SCIAMACHY) and Four Corners (−0.77 and −1.61 ppm) and a positive station bias e.g. at Garmisch (0.52 and 0.98 ppm). These similarities result in a high correlation coefficient of 0.83 between the station biases of SCIAMACHY BESD and GOSAT BESD (considering all stations with a sufficient number of collocations). The standard deviation of the difference at Karlsruhe is in both data sets similarly high (2.67 and 2.55 ppm) and similarly low at Darwin (1.24 ppm for GOSAT and 1.67 ppm for SCIAMACHY).

Overall, the analysis results for the time period 2010–2011 are similar to the results obtained for the full data set analysis. In both comparisons, the mean offset is negative (−0.42 ppm for GOSAT and −0.08 ppm for SCIAMACHY), the single measurement precision is similar (2.04 ppm for GOSAT and 2.12 ppm for SCIAMACHY) and the mean correlation coefficient is high (0.71 for GOSAT and 0.63 for SCIAMACHY). The station-to-station bias is slightly better for GOSAT with 0.48 ppm compared to 0.88 ppm for SCIAMACHY.

Results of the comparison of daily means of GOSAT BESD, SCIAMACHY BESD and TCCON XCO_2 are shown in Fig. 6. The daily means are computed using only days with more than three measurements within the $10^\circ \times 10^\circ$ around the TCCON sites. Figure 6 shows (similar to Fig. 5) (a) all collocated daily means of GOSAT and TCCON XCO_2 data between 2010 and 2011, (b) all collocated daily means of SCIAMACHY and TCCON XCO_2 data between 2010 and 2011 and additionally (c) all collocated daily means of GOSAT and SCIAMACHY XCO_2. The mean daily difference (offset) from TCCON is −0.34 ppm for GOSAT and 0.10 ppm for SCIAMACHY. The offset between the

Table 7. Results of the comparison of daily averages of (standard) GOSAT, SCIAMACHY and TCCON XCO_2 for 2010–2011 (see Fig. S3 for time series). The values are computed as for Table 6. Here, the comparisons at the TCCON sites marked with a *, with less than 10 days of data for all three comparisons, should be interpreted with care. The mean offset (mean of the mean differences), the estimated single measurement precision (mean of the standard deviation of the difference), the mean correlation coefficient and the station-to-station bias (standard deviation of the mean differences) are calculated without these stations.

Station	GOSAT–TCCON				SCIAMACHY–TCCON				GOSAT–SCIAMACHY			
	Δ [ppm]	σ [ppm]	r [–]	n [–]	Δ [ppm]	σ [ppm]	r [–]	n [–]	Δ [ppm]	σ [ppm]	r [–]	n [–]
Sodankylä*	–	–	–	2	1.26	1.24	0.94	23	–	–	–	0
Białystok	−0.33	1.58	0.85	13	0.10	1.80	0.82	39	−1.64	1.06	0.95	13
Bremen*	−0.65	1.66	0.72	11	−0.34	1.57	0.80	31	−0.74	2.05	0.76	8
Karlsruhe	−0.01	1.75	0.81	25	−0.05	1.89	0.78	81	−0.73	1.74	0.83	14
Orleans	0.51	1.70	0.87	14	0.72	1.76	0.70	40	−0.46	1.53	0.87	18
Garmisch	0.50	1.22	0.90	25	1.13	1.92	0.67	70	−1.03	1.65	0.85	15
Park Falls	0.38	0.75	0.96	19	0.93	1.30	0.88	86	−1.04	1.66	0.84	11
Four Corners	−0.70	1.56	0.78	55	−1.40	1.40	0.68	35	0.36	1.76	0.79	43
Lamont	−0.52	1.27	0.87	101	−0.37	1.75	0.72	227	−0.32	1.41	0.83	65
Tsukuba*	–	–	–	1	4.49	0.88	0.99	4	–	–	–	0
JPL*	–	–	–	3	−0.05	1.39	−0.14	4	−0.64	1.31	0.81	52
Saga*	–	–	–	1	−0.04	1.82	0.02	5	–	–	–	1
Izaña*	−0.52	1.58	0.54	9	–	–	–	0	–	–	–	0
Darwin	−0.95	0.64	0.79	22	−0.95	1.11	0.76	51	−1.30	1.12	0.64	40
Wollongong	−0.43	1.00	0.86	42	0.36	1.50	0.54	99	−0.76	1.67	0.61	35
Lauder*	0.37	1.30	0.84	5	–	–	–	1	–	–	–	0
MEAN	−0.17	1.28	0.85		−0.05	1.60	0.73		−0.77	1.51	0.80	
SD	0.54				0.85				0.59			

GOSAT and SCIAMACHY data is small with −0.60 ppm. The standard deviation of the daily difference to TCCON is for GOSAT smaller with 1.37 ppm compared to SCIAMACHY with 1.79 ppm. The standard deviation of the daily difference between GOSAT and SCIAMACHY is 1.56 ppm, which is similar to the comparison to TCCON. The correlation coefficient between GOSAT/TCCON is higher (0.86) compared to SCIAMACHY/TCCON (0.75) and similar to GOSAT/SCIAMACHY (0.82).

A more detailed comparison is shown in Table 7. Only stations with more than 10 days of data are used to compute the mean values shown in Table 7. The comparison with TCCON shows for GOSAT and SCIAMACHY BESD a small negative offset of −0.17 ppm (GOSAT) and −0.05 ppm (SCIAMACHY), a daily precision of 1.28 ppm (GOSAT) and 1.60 ppm (SCIAMACHY), a mean correlation coefficient of 0.85 (GOSAT) and 0.73 (SCIAMACHY) and a station-to-station bias of 0.54 ppm (GOSAT) and 0.85 ppm (SCIAMACHY). The correlation of the daily station biases at the TCCON sites for SCIAMACHY and GOSAT BESD is high ($r = 0.88$). The direct comparison between the GOSAT BESD and SCIAMACHY BESD XCO_2 data set shows that the satellite data have a −0.77 ppm offset against one another. However, this can be simply adjusted by accounting for this offset. The mean scatter of the differences of 1.51 ppm and the mean correlation coefficient of 0.80 are similar to the precision and mean correlation coefficient obtained by the comparison with TCCON. The standard deviation of the mean differences between GOSAT and SCIAMACHY of 0.59 ppm is smaller/similar than the station-to-station bias of daily GOSAT BESD and SCIAMACHY BESD data.

The differences between the satellite data are likely due to non-perfect collocations (observed air masses are not identical) and potentially due to a non-perfect BESD retrieval algorithm. However, the similar scatter of the difference between the data sets compared to the difference to TCCON, the high correlation coefficient of the station biases and the smaller/similar standard deviation of the mean differences of the data sets compared to the station-to-station bias indicate a high degree of consistency between the SCIAMACHY and GOSAT XCO_2 data sets.

7 Comparisons with CarbonTracker XCO_2

In addition to the comparisons with TCCON, we have also compared the BESD data sets with the model results of CarbonTracker. For this purpose, we have used data of 4 months in 2011: we selected April–May when the atmospheric CO_2 concentration in the Northern Hemisphere peaks and August–September where it reaches its minimum.

CarbonTracker is NOAA's modelling and assimilation system and has been developed to estimate global CO_2 concentrations and CO_2 surface fluxes (Peters et al., 2007). We use CarbonTracker version CT2013B downloaded from http://carbontracker.noaa.gov. Global monthly maps of GOSAT

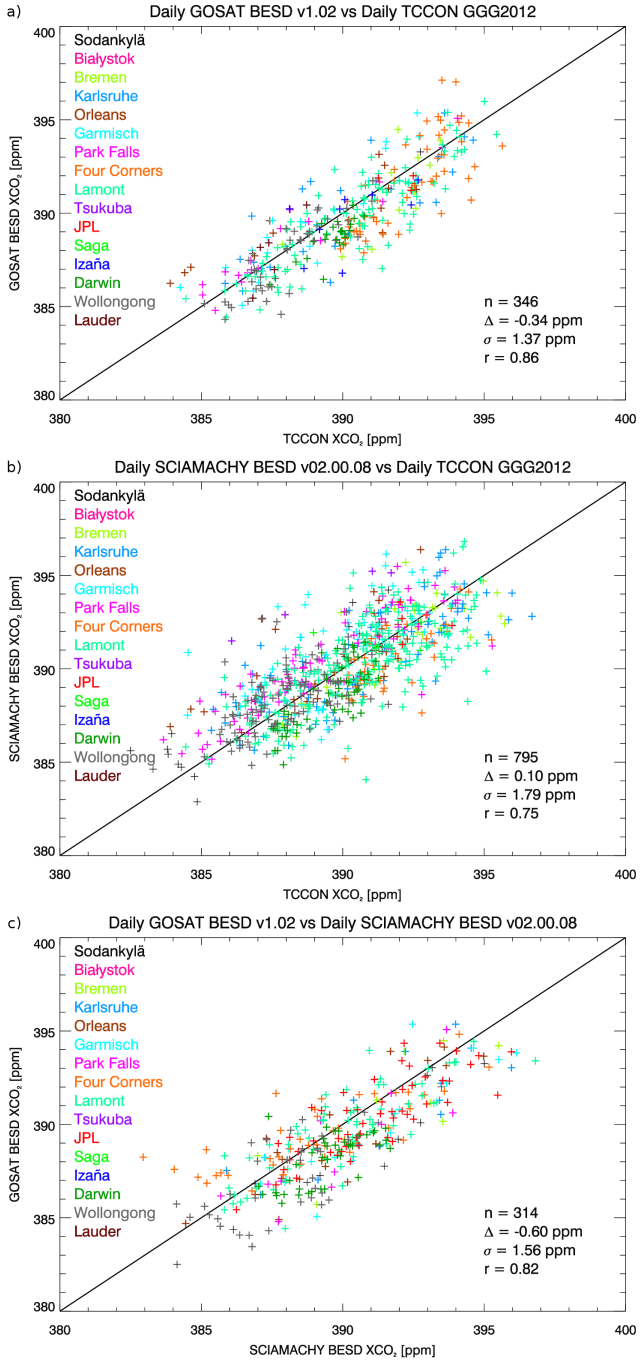

Figure 6. As Fig. 5 but for daily averages of GOSAT, SCIAMACHY and TCCON XCO_2 (2010–2011). **(a)** GOSAT BESD XCO_2 vs. TCCON XCO_2. **(b)** SCIAMACHY BESD XCO_2 vs. TCCON XCO_2. **(c)** GOSAT BESD XCO_2 vs. SCIAMACHY BESD XCO_2.

BESD, SCIAMACHY BESD and CarbonTracker XCO_2 have been generated in a grid of $5° \times 5°$. All grid boxes with less than 15 measurements have been excluded to achieve robust results. A global mean offset has been added to GOSAT BESD (1 ppm) and SCIAMACHY BESD (0.4 ppm) to better compare the differences to CarbonTracker. From the intercomparison of the global maps the mean difference, the standard deviation of the difference and the correlation coefficient between the data sets have been computed.

Figure 7 shows the comparison results for April–May 2011. The GOSAT BESD, SCIAMACHY BESD and CarbonTracker maps show a similar strong latitudinal dependence of XCO_2 with high XCO_2 in the Northern Hemisphere and low XCO_2 in the Southern Hemisphere. The number of grid boxes filled with sufficient observations is larger for SCIAMACHY than for GOSAT BESD. In comparison to CarbonTracker, GOSAT BESD as well as SCIAMACHY BESD has a small mean difference (GOSAT: 0.10 ppm; SCIAMACHY: 0.03 ppm) and a similar standard deviation of the difference (GOSAT: 1.29 ppm; SCIAMACHY: 1.30 ppm). The correlation coefficient between the BESD data sets and CarbonTracker is similarly high (~ 0.9). The direct comparison between GOSAT BESD and SCIAMACHY BESD shows a mean difference of 0.09 ppm, a smaller standard deviation of the difference of 1.17 ppm and a similar correlation coefficient ($r = 0.92$) as compared to the difference to CarbonTracker. In addition to the global maps, latitudinal averages of the differences are shown (Fig. 7, right panel). Generally the latitudinal differences between the data sets are small. We have also computed the standard deviation of the latitudinal differences (σ_l). The differences between GOSAT BESD or SCIAMACHY BESD to CarbonTracker show a similar σ_l (GOSAT: 0.42 ppm; SCIAMACHY: 0.44 ppm), but the differences between GOSAT and SCIAMACHY BESD are smaller with $\sigma_l = 0.29$ ppm. These results show that the north to south dependence of XCO_2 is more consistent between the BESD data sets as compared to CarbonTracker.

The results for August–September 2011 are shown in Fig. 8. The northern hemispheric carbon uptake in this time period explains the low XCO_2 values in the Northern Hemisphere shown in all three data sets. The number of grid boxes is again larger for SCIAMACHY compared to GOSAT BESD. The comparison with CarbonTracker shows for GOSAT and SCIAMACHY a similar small offset (-0.04 ppm). The standard deviation of the difference is somewhat smaller for GOSAT (1.14 ppm) as compared to SCIAMACHY BESD (1.28 ppm) and the correlation coefficient is similar (GOSAT: 0.71; SCIAMACHY: 0.74). The direct comparison of the BESD data sets shows a smaller/similar standard deviation of the difference (1.02 ppm) and has a similarly high correlation coefficient (0.80) as obtained from the comparison with CarbonTracker. The latitudinal averages of GOSAT BESD–CarbonTracker as well as SCIAMACHY BESD–CarbonTracker decrease in a similar way near the equator. As a result the latitudinal averages of the difference between the two BESD data sets are smaller ($\sigma_l = 0.35$ ppm) than the difference of either data set to CarbonTracker (GOSAT: 0.68 ppm; SCIA-

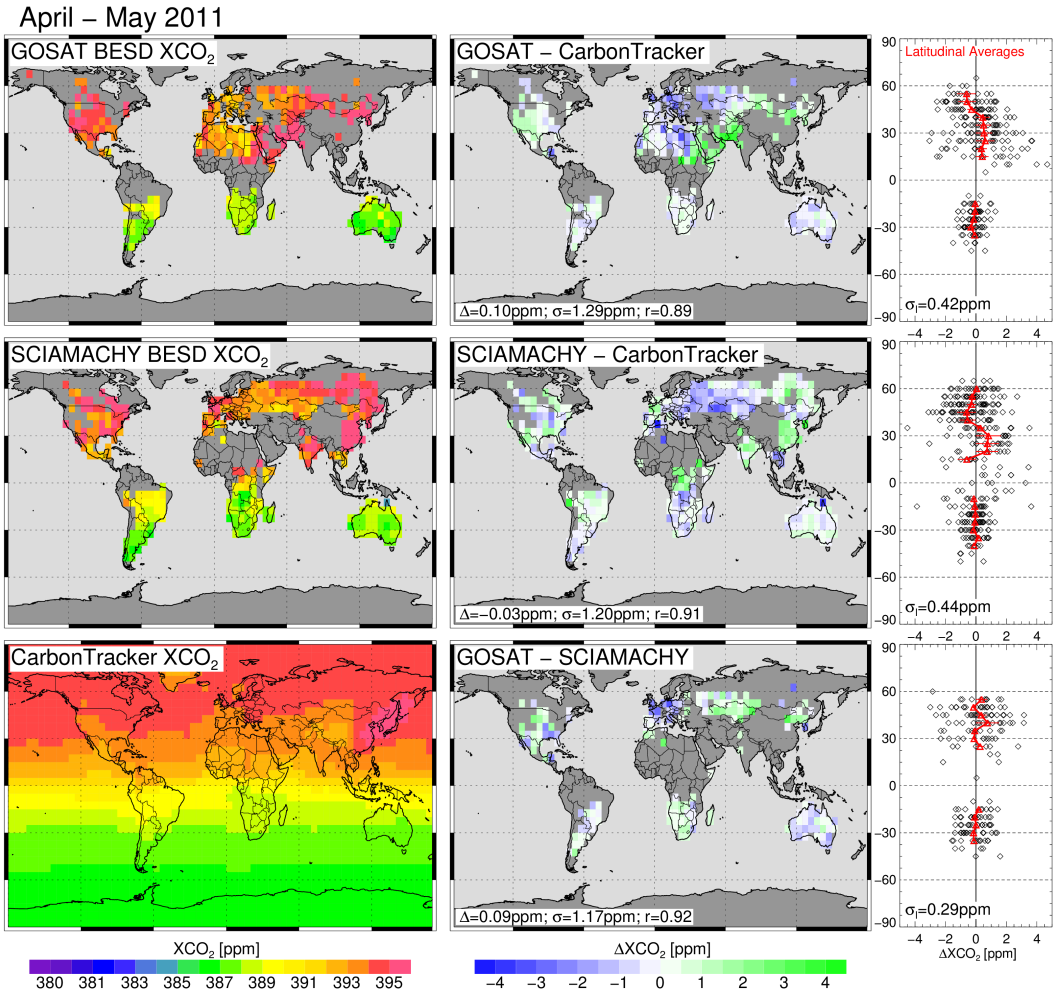

Figure 7. Global maps of XCO_2 (left), XCO_2 differences (ΔXCO_2, middle) and latitudinal averages of the differences (right) of GOSAT BESD, SCIAMACHY BESD and CarbonTracker gridded on $5^\circ \times 5^\circ$ for April–May 2011. The values shown near the bottom of the difference maps are Δ, the mean difference between the data products, σ, the standard deviation of the difference and r, the correlation coefficient. The black diamonds in the right panels are the XCO_2 differences in the individual grid boxes. The red triangles represent the latitudinal averages and the error bars the latitudinal standard deviation. σ_l is the standard deviation over all latitudinal averages.

MACHY: 0.62 ppm). These results again show that the north to south dependence of XCO_2 is more consistent between the BESD data sets as compared to CarbonTracker.

The remaining differences between GOSAT and SCIAMACHY BESD are likely due to the non-perfect spatial and temporal collocations and a non-perfect BESD algorithm. However, the smaller/similar differences of the BESD data sets as compared to CarbonTracker are another indication for the high degree of consistency between GOSAT and SCIAMACHY BESD.

8 Conclusions

As consistent long-term data sets of XCO_2 are required for carbon cycle and climate-related research, we have investigated whether retrievals of XCO_2 from different satellites but evaluated using the same retrieval algorithm are consistent. For this purpose, the BESD algorithm originally developed for SCIAMACHY measurements has been modified and used to also evaluate GOSAT measurements.

The quality of the BESD data products was estimated by a validation study using TCCON observations. This comparison showed that the GOSAT BESD XCO_2 data product has a mean offset of -0.30 ppm, a single measurement precision of 2.09 ppm, a mean correlation coefficient of 0.79 and a station-to-station bias of 0.43 ppm. The SCIAMACHY BESD XCO_2 data product has a mean offset of -0.05 ppm, a single measurement precision of 2.20 ppm, a mean correlation coefficient of 0.78 and a station-to-station bias of 0.89 ppm (0.67 ppm without Four Corners).

In order to evaluate the consistency of the satellite data products, we compared the data products with the TCCON

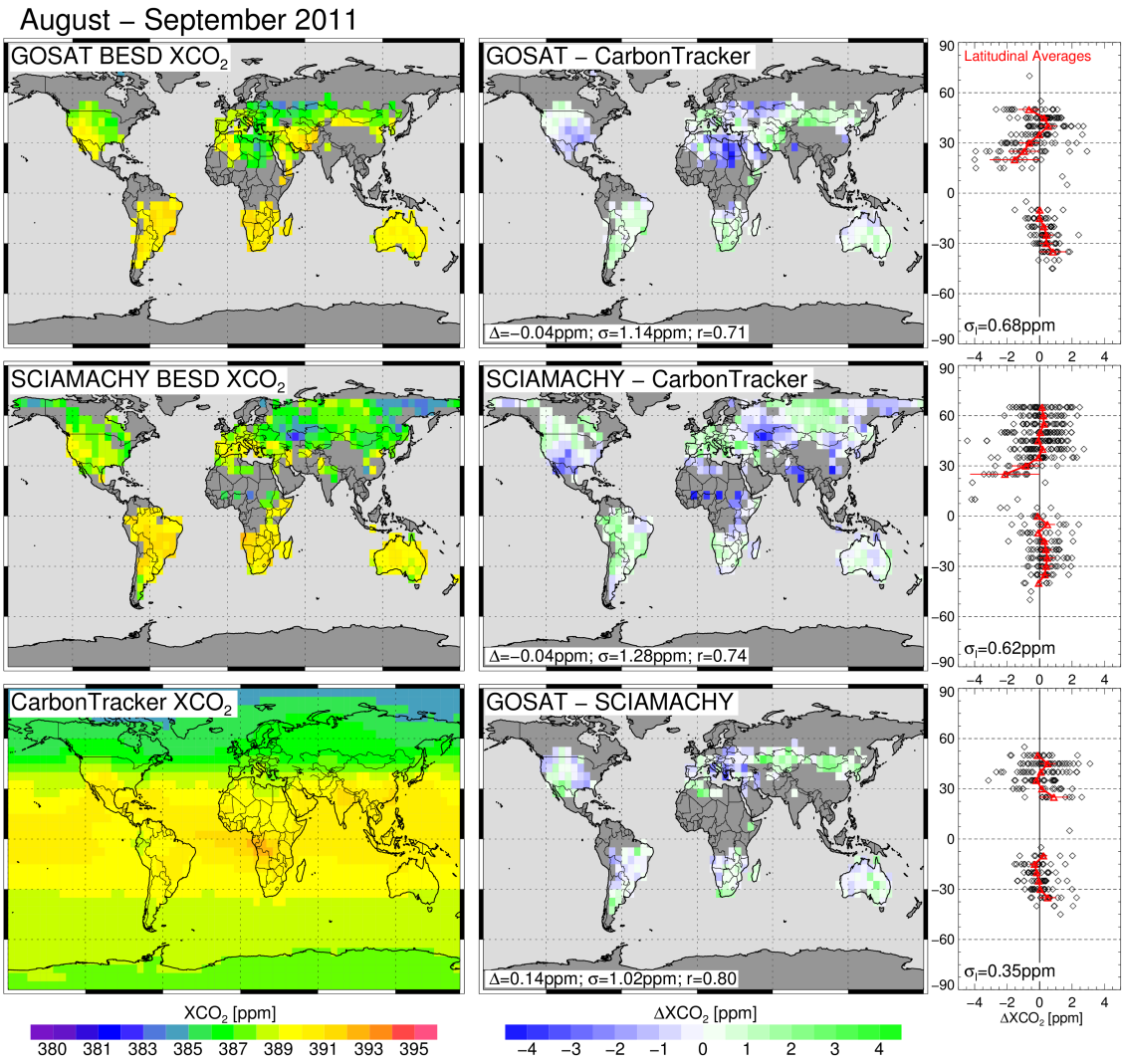

Figure 8. As Fig. 7 but for August–September 2011.

data for the same time period and performed a direct comparison of the satellite data.

The comparison of the validation results for the years 2010–2011, when the observation periods of SCIAMACHY and GOSAT overlap, showed for both data sets a small mean offset (−0.42 ppm for GOSAT, −0.08 ppm for SCIAMACHY), a similar single measurement precision of 2.04 ppm for GOSAT and 2.12 ppm for SCIAMACHY and a similar mean correlation coefficient for GOSAT (0.71) and SCIAMACHY (0.63). The station-to-station bias for GOSAT is slightly better with 0.48 ppm compared to 0.88 ppm for SCIAMACHY.

The GOSAT BESD and SCIAMACHY BESD XCO_2 data show similarities in the comparisons at the TCCON sites. The mean difference from TCCON is at e.g. Bremen (−1.01 ppm for GOSAT and −1.07 ppm for SCIAMACHY) and Darwin (−1.00 ppm for GOSAT and −0.87 ppm for SCIAMACHY) similarly low. Overall, the correlation coefficient between the station biases of both data sets is large (0.83). The single measurement precision has similar small values e.g. at Darwin (1.24 ppm for GOSAT and 1.67 ppm for SCIAMACHY) and a similar high value e.g. at Karlsruhe (2.67 ppm for GOSAT and 2.55 ppm for SCIAMACHY). These similarities, the large correlation coefficient of the station biases and the similarity of the validation results give evidence that the GOSAT BESD XCO_2 and the SCIAMACHY BESD XCO_2 are generally consistent.

In a direct comparison of the satellite data, we analysed daily averages of GOSAT and SCIAMACHY BESD XCO_2. This analysis showed an offset between the data sets of −0.77 ppm, a similar standard difference between the data sets (1.51 ppm) compared to the TCCON comparison (1.28 ppm for GOSAT and 1.60 ppm for SCIAMACHY), a high correlation coefficient (0.80) and smaller/similar station-to-station variations of the mean dif-

ference (0.59 ppm) compared to the difference to TCCON (0.54 ppm for GOSAT and 0.85 ppm for SCIAMACHY).

We have also compared global monthly maps and latitudinal averages of the satellite data sets with CarbonTracker XCO_2. Results of two time periods, April–May and August–September 2011, were presented. These results showed that the differences between the BESD data sets are smaller/similar as the difference to CarbonTracker.

The remaining differences found between GOSAT and SCIAMACHY are likely not only due to non-perfect collocation (i.e. the observed air masses can be not identical) but likely also to a non-perfect BESD retrieval algorithm. However, the similar scatter of the difference between the data sets compared to the difference to TCCON and CarbonTracker and the smaller/similar station-to-station variation of the differences of the data sets compared to the difference to TCCON indicate a high degree of consistency between the SCIAMACHY and GOSAT XCO_2 data sets. These results demonstrates that consistent retrievals can be obtained from different satellite instruments using the same retrieval algorithm.

Our overarching goal is to generate a satellite-derived XCO_2 data set appropriate for climate and carbon cycle research covering the longest time period. We therefore also plan to extend the existing SCIAMACHY and GOSAT data set discussed here by also using data from other current or future missions, e.g. OCO-2 (Crisp et al., 2004), GOSAT-2 and CarbonSat (Bovensmann et al., 2010; Buchwitz et al., 2013a).

The Supplement related to this article is available online at doi:10.5194/amt-8-2961-2015-supplement.

Acknowledgements. We thank JAXA, NIES and ESA for providing us with the GOSAT L1B and L2 IDS data. We are also grateful to Jonathan de Ferranti for the development of the digital elevation model, which we used for our evaluations. We thank TCCON for providing FTS XCO_2 data obtained from the TCCON Data Archive, operated by the California Institute of Technology, from the website at http://tccon.ipac.caltech.edu/. The CarbonTracker CT2013B results has been provided by NOAA ESRL, Boulder, Colorado, USA, from the website at http://carbontracker.noaa.gov. We thank NASA for providing us with the ABSCOv4 tables and ECMWF for the meteorological data. This work has been funded by the EU FP7 (MACC-II), EU Horizon 2020 (MACC-III), ESA (GHG-CCI project and Living Planet Fellowship project CARBOFIRES) and the state and the University of Bremen.

The article processing charges for this open-access publication were covered by the University of Bremen.

Edited by: D. Brunner

References

Aben, I., Hasekamp, O., and Hartmann, W.: Uncertainties in the space-based measurements of CO_2 columns due to scattering in the Earth's atmosphere, J. Quant. Spectrosc. Ra., 104, 450–459, doi:10.1016/j.jqsrt.2006.09.013, 2006.

Agustí-Panareda, A., Massart, S., Chevallier, F., Boussetta, S., Balsamo, G., Beljaars, A., Ciais, P., Deutscher, N. M., Engelen, R., Jones, L., Kivi, R., Paris, J.-D., Peuch, V.-H., Sherlock, V., Vermeulen, A. T., Wennberg, P. O., and Wunch, D.: Forecasting global atmospheric CO_2, Atmos. Chem. Phys., 14, 11959–11983, doi:10.5194/acp-14-11959-2014, 2014.

Bovensmann, H., Burrows, J. P., Buchwitz, M., Frerick, J., Noël, S., Rozanov, V. V., Chance, K. V., and Goede, A.: SCIAMACHY – mission objectives and measurement modes, J. Atmos. Sci., 56, 127–150, 1999.

Bovensmann, H., Buchwitz, M., Burrows, J. P., Reuter, M., Krings, T., Gerilowski, K., Schneising, O., Heymann, J., Tretner, A., and Erzinger, J.: A remote sensing technique for global monitoring of power plant CO_2 emissions from space and related applications, Atmos. Meas. Tech., 3, 781–811, doi:10.5194/amt-3-781-2010, 2010.

Buchwitz, M., Rozanov, V. V., and Burrows, J. P.: A correlated-k distribution scheme for overlapping gases suitable for retrieval of atmospheric constituents from moderate resolution radiance measurements in the visible/near-infrared spectral region, J. Geophys. Res., 105, 15247–15261, 2000.

Buchwitz, M., Reuter, M., Bovensmann, H., Pillai, D., Heymann, J., Schneising, O., Rozanov, V., Krings, T., Burrows, J. P., Boesch, H., Gerbig, C., Meijer, Y., and Löscher, A.: Carbon Monitoring Satellite (CarbonSat): assessment of atmospheric CO_2 and CH_4 retrieval errors by error parameterization, Atmos. Meas. Tech., 6, 3477–3500, doi:10.5194/amt-6-3477-2013, 2013a.

Buchwitz, M., Reuter, R., Schneising, O., Bösch, H., Guerlet, S., Dils, B., Aben, I., Armante, R., Bergamaschi, P., Blumenstock, T., Bovensmann, H., Brunner, D., Buchmann, B., Burrows, J. P., Butz, A., Chedin, A., Chevallier, F., Crevoisier, C. D., Deutscher, N. M., Frankenberg, C., Hase, F., Hasekamp, O. P., Heymann, J., Kaminski, T., Laeng, A., Lichtenberg, G., De Maziere, M., Noel, S., Notholt, J., Orphal, J., Popp, C., Parker, R., Scholze, M., Sussmann, R. Stiller, G. P., Warneke, T., Zehner, C., Bril, A., Crisp, D., Griffith, D. W. T. Kuze, A., O'Dell, D. W. T., Oshchepkov, S., Sherlock, V., Suto, H., Wennberg, P., Wunch, D., Yokota, T., and Yoshida, Y.: The Greenhouse Gas Climate Change Initiative (GHG-CCI): comparison and quality assessment of near-surface-sensitive satellite-derived CO_2 and CH_4 global data sets, Remote Sens. Environ., online first, doi:10.1016/j.rse.2013.04.024, 2013b.

Burrows, J. P., Hölzle, E., Goede, A. P. H., Visser, H., and Fricke, W.: SCIAMACHY – Scanning Imaging Absorption Spectrometer for Atmospheric Chartography, Acta Astronaut., 35, 445–451, 1995.

Butz, A., Guerlet, S., Hasekamp, O., Schepers, D., Galli, A., Aben, I., Frankenberg, C., Hartmann, J.-M., Tran, H., Kuze, A., Keppel-Aleks, G., Toon, G., Wunch, D., Wennberg, P., Deutscher, N., Griffith, D., Macatangay, R., Messerschmidt, J., Notholt, J., and Warneke, T.: Toward accurate CO_2 and CH_4 observations from GOSAT, Geophys. Res. Lett., 38, L14812, doi:10.1029/2011GL047888, 2011.

Chevallier, F., Bréon, F.-M., and Rayner, P. J.: Contribution of the orbiting carbon observatory to the estimation of CO_2 sources and sinks: theoretical study in a variational data assimilation framework, J. Geophys. Res., 112, D09307, doi:10.1029/2006JD007375, 2007.

Cogan, A. J., Bösch, H., Parker, R. J., Feng, L., Palmer, P. I., Blavier, J.-F. L., Deutscher, N. M., Macatangay, R., Norholt, J., Roehl, C., Warneke, T., and Wunch, D.: Atmospheric carbon dioxide retrieved from the Greenhouse gases Observing SATellite (GOSAT): comparison with ground-based TCCON obserations and GEOS-Chem model calculations, J. Geophys. Res., 117, D21301, doi:10.1029/2012JD018087, 2012.

Crisp, D., Atlas, R. M., Bréon, F.-M., Brown, L. R., Burrows, J. P., Ciais, P., Connor, B. J., Doney, S. C., Fung, I. Y., Jacob, D. J., Miller, C. E., O'Brien, D., Pawson, S., Randerson, J. T., Rayner, P., Salawitch, R. S., Sander, S. P., Sen, B., Stephens, G. L., Tans, P. P., Toon, G. C., Wennberg, P. O., Wofsy, S. C., Yung, Y. L., Kuang, Z., Chudasama, B., Sprague, G., Weiss, P., Pollock, R., Kenyon, D., and Schroll, S.: The Orbiting Carbon Observatory (OCO) mission, Adv. Space Res., 34, 700–709, 2004.

Crisp, D., Fisher, B. M., O'Dell, C., Frankenberg, C., Basilio, R., Bösch, H., Brown, L. R., Castano, R., Connor, B., Deutscher, N. M., Eldering, A., Griffith, D., Gunson, M., Kuze, A., Mandrake, L., McDuffie, J., Messerschmidt, J., Miller, C. E., Morino, I., Natraj, V., Notholt, J., O'Brien, D. M., Oyafuso, F., Polonsky, I., Robinson, J., Salawitch, R., Sherlock, V., Smyth, M., Suto, H., Taylor, T. E., Thompson, D. R., Wennberg, P. O., Wunch, D., and Yung, Y. L.: The ACOS CO_2 retrieval algorithm – Part II: Global XCO_2 data characterization, Atmos. Meas. Tech., 5, 687–707, doi:10.5194/amt-5-687-2012, 2012.

Dee, D. P., Uppala, S. M., Simmons, A. J., Berrisford, P., Poli, P., Kobayashi, S., Andrae, U., Balmaseda, M. A., Balsamo, G., Bauer, P., Bechtold, P., Beljaars, A. C. M., van de Berg, L., Bidlot, J., Bormann, N., Delsol, C., Dragani, R., Fuentes, M., Geer, A. J., Haimberger, L., H. S. B., Hersbach, H., Hólm, E. V., Isaksen, L., Kållberg, P., Köhler, M., Matricardi, M., McNally, A. P., Monge-Sanz, B. M., Morcrette, J.-J., Park, B.-K., Peubey, C., de Rosnay, P., Tavolato, C., Thépaut, J.-N., and Vitart, F.: The ERA-Interim reanalysis: configuration and performance of the data assimilation system, Q. J. Roy. Meteor. Soc., 137, 553–597, doi:10.1002/qj.828, 2011.

Dils, B., Buchwitz, M., Reuter, M., Schneising, O., Boesch, H., Parker, R., Guerlet, S., Aben, I., Blumenstock, T., Burrows, J. P., Butz, A., Deutscher, N. M., Frankenberg, C., Hase, F., Hasekamp, O. P., Heymann, J., De Mazière, M., Notholt, J., Sussmann, R., Warneke, T., Griffith, D., Sherlock, V., and Wunch, D.: The Greenhouse Gas Climate Change Initiative (GHG-CCI): comparative validation of GHG-CCI SCIAMACHY/ENVISAT and TANSO-FTS/GOSAT CO_2 and CH_4 retrieval algorithm products with measurements from the TCCON, Atmos. Meas. Tech., 7, 1723–1744, doi:10.5194/amt-7-1723-2014, 2014.

Guerlet, S., Butz, A., Schepers, D., Basu, S., Hasekamp, O. P., Kuze, A., Yokota, T., Blavier, J., Deutscher, N. M., Griffith, D. W. T., Hase, F., Kyro, E., Morino, I., Sherlock, V., Sussmann, R., Galli, A., and Aben, I.: Impact of aerosol and thin cirrus on retrieving and validating XCO_2 from GOSAT shortwave infrared measurements, J. Geophys. Res., 118, 4887–4905, doi:10.1002/jgrd.50332, 2013.

Heymann, J., Schneising, O., Reuter, M., Buchwitz, M., Rozanov, V. V., Velazco, V. A., Bovensmann, H., and Burrows, J. P.: SCIAMACHY WFM-DOAS XCO_2: comparison with CarbonTracker XCO_2 focusing on aerosols and thin clouds, Atmos. Meas. Tech., 5, 1935–1952, doi:10.5194/amt-5-1935-2012, 2012a.

Heymann, J., Bovensmann, H., Buchwitz, M., Burrows, J. P., Deutscher, N. M., Notholt, J., Rettinger, M., Reuter, M., Schneising, O., Sussmann, R., and Warneke, T.: SCIAMACHY WFM-DOAS XCO_2: reduction of scattering related errors, Atmos. Meas. Tech., 5, 2375–2390, doi:10.5194/amt-5-2375-2012, 2012b.

Hilker, M.: Influence of the linear-k method on the accuracy and computational efficiency of GOSAT XCO_2 retrievals, Atmos. Meas. Tech., in preparation, 2015.

Hollingsworth, A., Engelen, R. J., Benedetti, A., Dethof, A., Flemming, J., Kaiser, J. W., Morcrette, J.-J., Simmons, A. J., Textor, C., Boucher, O., Chevallier, F., Rayner, P., Elbern, H., Eskes, H., Granier, C., Peuch, V.-H., Rouil, L., and Schultz, M. G.: Toward a monitoring and forecasting system for atmospheric composition: the GEMS project, B. Am. Meteorol. Soc., 89, 1147–1164, 2008.

Hollmann, R., Merchant, C. J., Saunders, R., Downy, C., Buchwitz, M., Cazenave, A., Chuvieco, E., Defourny, P., de Leeuw, G., Forsberg, R., Holzer-Popp, T., Paul, F., Sandven, S., Sathyendranath, S., van Roozendael, M., and Wagner, W.: The ESA climate change initiative: satellite data records for essential climate variables, B. Am. Meteorol. Soc., 94, 1541–1552, doi:10.1175/BAMS-D-11-00254.1, 2013.

Houweling, S., Breon, F.-M., Aben, I., Rödenbeck, C., Gloor, M., Heimann, M., and Ciais, P.: Inverse modeling of CO_2 sources and sinks using satellite data: a synthetic inter-comparison of measurement techniques and their performance as a function of space and time, Atmos. Chem. Phys., 4, 523–538, doi:10.5194/acp-4-523-2004, 2004.

Houweling, S., Hartmann, W., Aben, I., Schrijver, H., Skidmore, J., Roelofs, G.-J., and Breon, F.-M.: Evidence of systematic errors in SCIAMACHY-observed CO_2 due to aerosols, Atmos. Chem. Phys., 5, 3003–3013, doi:10.5194/acp-5-3003-2005, 2005.

Hungershoefer, K., Breon, F.-M., Peylin, P., Chevallier, F., Rayner, P., Klonecki, A., Houweling, S., and Marshall, J.: Evaluation of various observing systems for the global monitoring of CO_2 surface fluxes, Atmos. Chem. Phys., 10, 10503–10520, doi:10.5194/acp-10-10503-2010, 2010.

Kuze, A., Suto, H., Nakajima, M., and Hamazaki, T.: Thermal and near infrared sensor for carbon observation Fourier-transform spectrometer on the Greenhouse Gases Observing Satellite for greenhouse gases monitoring, Appl. Optics, 48, 6716–6733, 2009.

Lindenmaier, R., Dubey, M. K., Henderson, B. G., Zachary, T. B., Herman, J. R., Rahn, T., and Lee, S.-H.: Multiscale observations of CO_2, $^{13}CO_2$, and pollutants at Four Corners for emission verification and attribution, P. Natl. Acad. Sci. USA, 111, 8386–8391, doi:10.1073/pnas.1321883111, 2014.

Messerschmidt, J., Geibel, M. C., Blumenstock, T., Chen, H., Deutscher, N. M., Engel, A., Feist, D. G., Gerbig, C., Gisi, M., Hase, F., Katrynski, K., Kolle, O., Lavrič, J. V., Notholt, J.,

Palm, M., Ramonet, M., Rettinger, M., Schmidt, M., Sussmann, R., Toon, G. C., Truong, F., Warneke, T., Wennberg, P. O., Wunch, D., and Xueref-Remy, I.: Calibration of TCCON column-averaged CO_2: the first aircraft campaign over European TCCON sites, Atmos. Chem. Phys., 11, 10765–10777, doi:10.5194/acp-11-10765-2011, 2011.

Miller, C. E., Crisp, D., DeCola, P. L., Olsen, S. C., Randerson, J. T., Michalak, A. M., Alkhaled, A., Rayner, P., Jacob, D. J., Suntharalingam, P., Jones, D. B. A., Denning, A. S., Nicholls, M. E., Doney, S. C., Pawson, S., Boesch, H., Connor, B. J., Fung, I. Y., O'Brien, D., Salawitch, R. J., Sander, S. P., Sen, B., Tans, P., Toon, G. C., Wennberg, P. O., Wofsy, S. C., Yung, Y. L., and Law, R. M.: Precision requirements for space-based X_{CO_2} data, J. Geophys. Res., 112, D10314, doi:10.1029/2006JD007659, 2007.

O'Dell, C. W., Connor, B., Bösch, H., O'Brien, D., Frankenberg, C., Castano, R., Christi, M., Eldering, D., Fisher, B., Gunson, M., McDuffie, J., Miller, C. E., Natraj, V., Oyafuso, F., Polonsky, I., Smyth, M., Taylor, T., Toon, G. C., Wennberg, P. O., and Wunch, D.: The ACOS CO_2 retrieval algorithm – Part 1: Description and validation against synthetic observations, Atmos. Meas. Tech., 5, 99–121, doi:10.5194/amt-5-99-2012, 2012.

Oshchepkov, S., Bril, A., and Yokota, T.: PPDF-based method to account for atmospheric light scattering in observations of carbon dioxide from space, J. Geophys. Res.-Atmos., 113, D23210, doi:10.1029/2008JD010061, 2008.

Peters, W., Jacobson, A. R., Sweeney, C., Andrews, A. E., Conway, T. J., Masarie, K., Miller, J. B., Bruhwiler, L. M. P., Petron, G., Hirsch, A. I., Worthy, D. E. J., van der Werf, G. R., Randerson, J. T., Wennberg, P. O., Krol, M. C., and Tans, P. P.: An atmospheric perspective on North American carbon dioxide exchange: CarbonTracker, P. Natl. Acad. Sci. USA, 104, 18925–18930, doi:10.1073/pnas.0708986104, 2007.

Rayner, P. J. and O'Brien, D. M.: The utility of remotely sensed CO_2 concentration data in surface inversions, Geophys. Res. Lett., 28, 175–178, 2001.

Reuter, M., Buchwitz, M., Schneising, O., Heymann, J., Bovensmann, H., and Burrows, J. P.: A method for improved SCIAMACHY CO_2 retrieval in the presence of optically thin clouds, Atmos. Meas. Tech., 3, 209–232, doi:10.5194/amt-3-209-2010, 2010.

Reuter, M., Bovensmann, H., Buchwitz, M., Burrows, J. P., Connor, B. J., Deutscher, N. M., Griffith, D. W. T., Heymann, J., Keppel-Aleks, G., Messerschmidt, J., Notholt, J., Petri, C., Robinson, J., Schneising, O., Sherlock, V., Velazco, V., Warneke, T., Wennberg, P. O., and Wunch, D.: Retrieval of atmospheric CO_2 with enhanced accuracy and precision from SCIAMACHY: validation with FTS measurements and comparison with model results, J. Geophys. Res., 116, D04301, doi:10.1029/2010JD015047, 2011.

Reuter, M., Bovensmann, H., Buchwitz, M., Burrows, J., Deutscher, N., Heymann, J., Rozanov, A., Schneising, O., Suto, H., Toon, G., and Warneke, T.: On the potential of the 2041–2047 nm spectral region for remote sensing of atmospheric CO_2 isotopologues, J. Quant. Spectrosc. Ra., 12, 2009–2017, 2012a.

Reuter, M., Buchwitz, M., Schneising, O., Hase, F., Heymann, J., Guerlet, S., Cogan, A. J., Bovensmann, H., and Burrows, J. P.: A simple empirical model estimating atmospheric CO_2 background concentrations, Atmos. Meas. Tech., 5, 1349–1357, doi:10.5194/amt-5-1349-2012, 2012b.

Reuter, M., Bösch, H., Bovensmann, H., Bril, A., Buchwitz, M., Butz, A., Burrows, J. P., O'Dell, C. W., Guerlet, S., Hasekamp, O., Heymann, J., Kikuchi, N., Oshchepkov, S., Parker, R., Pfeifer, S., Schneising, O., Yokota, T., and Yoshida, Y.: A joint effort to deliver satellite retrieved atmospheric CO_2 concentrations for surface flux inversions: the ensemble median algorithm EMMA, Atmos. Chem. Phys., 13, 1771–1780, doi:10.5194/acp-13-1771-2013, 2013.

Reuter, M., Bovensmann, H., Buchwitz, M., Burrows, J. P., Heymann, J., Hilker, M., and Schneising, O.: Algorithm Theoretical Basis Document Version 3 – The Bremen Optimal Estimation DOAS (BESD) algorithm for the retrieval of XCO_2 – ESA Climate Change Initiative (CCI) for the Essential Climate Variable (ECV), Tech. rep., University of Bremen, available at: http://www.esa-ghg-cci.org (last access: 18 December 2014), 2014a.

Reuter, M., Buchwitz, M., Hilboll, A., Richter, A., Schneising, O., Hilker, M., Heymann, J., Bovensmann, H., and Burrows, J. P.: Decreasing emissions of NO_x relative to CO_2 in East Asia inferred from satellite observations, Nat. Geosci., 7, 792–795, doi:10.1038/ngeo2257, 2014b.

Reuter, M., Buchwitz, M., Hilker, M., Heymann, J., Schneising, O., Pillai, D., Bovensmann, H., Burrows, J. P., Bösch, H., Parker, R., Butz, A., Hasekamp, O., O'Dell, C. W., Yoshida, Y., Gerbig, C., Nehrkorn, T., Deutscher, N. M., Warneke, T., Notholt, J., Hase, F., Kivi, R., Sussmann, R., Machida, T., Matsueda, H., and Sawa, Y.: Satellite-inferred European carbon sink larger than expected, Atmos. Chem. Phys., 14, 13739–13753, doi:10.5194/acp-14-13739-2014, 2014c.

Rodgers, C. D.: Inverse Methods for Atmospheric Sounding: Theory and Practice, World Scientific Publishing, Singapore, 2000.

Rothman, L. S., Gordon, I. E., Barbe, A., Benner, D. C., Bernath, P. E., Birk, M., Boudon, V., Brown, L. R., Campargue, A., Champion, J. P., Chance, K., Coudert, L. H., Dana, V., Devi, V. M., Fally, S., Flaud, J. M., Gamache, R. R., Goldman, A., Jacquemart, D., Kleiner, I., Lacome, N., Lafferty, W. J., Mandin, J. Y., Massie, S. T., Mikhailenko, S. N., Miller, C. E., Moazzen-Ahmadi, N., Naumenko, O. V., Nikitin, A. V., Orphal, J., Perevalov, V. I., Perrin, A., Predoi-Cross, A., Rinsland, C. P., Rotger, M., Simeckova, M., Smith, M. A. H., Sung, K., Tashkun, S. A., Tennyson, J., Toth, R. A., Vandaele, A. C., and Vander Auwera, J.: The HITRAN 2008 molecular spectroscopic database, J. Quant. Spectrosc. Ra., 110, 533–572, doi:10.1016/j.jqsrt.2009.02.013, 2009.

Rozanov, V. V., Rozanov, A., Kokhanovsky, A. A., and Burrows, J. P.: Radiative transfer through terrestrial atmosphere and ocean: software package SCIATRAN, J. Quant. Spectrosc. Ra., 133, 13–71, doi:10.1016/j.jqsrt.2013.07.004, 2014.

Schneising, O., Bergamaschi, P., Bovensmann, H., Buchwitz, M., Burrows, J. P., Deutscher, N. M., Griffith, D. W. T., Heymann, J., Macatangay, R., Messerschmidt, J., Notholt, J., Rettinger, M., Reuter, M., Sussmann, R., Velazco, V. A., Warneke, T., Wennberg, P. O., and Wunch, D.: Atmospheric greenhouse gases retrieved from SCIAMACHY: comparison to ground-based FTS measurements and model results, Atmos. Chem. Phys., 12, 1527–1540, doi:10.5194/acp-12-1527-2012, 2012.

Schneising, O., Heymann, J., Buchwitz, M., Reuter, M., Bovensmann, H., and Burrows, J. P.: Anthropogenic carbon dioxide

source areas observed from space: assessment of regional enhancements and trends, Atmos. Chem. Phys., 13, 2445–2454, doi:10.5194/acp-13-2445-2013, 2013.

Schneising, O., Reuter, M., Buchwitz, M., Heymann, J., Bovensmann, H., and Burrows, J. P.: Terrestrial carbon sink observed from space: variation of growth rates and seasonal cycle amplitudes in response to interannual surface temperature variability, Atmos. Chem. Phys., 14, 133–141, doi:10.5194/acp-14-133-2014, 2014.

Takagi, H., Houweling, S., Andres, R. J., Belikov, D., Bril, A., Boesch, H., Butz, A., Guerlet, S., Hasekamp, O., Maksyutov, S., Morino, I., Oda, T., O'Dell, C. W., Oshchepkov, S., Parker, R., Saito, M., Uchino, O., Yokota, T., Yoshida, Y., and Valsala, V.: Influence of differences in current GOSAT XCO_2 retrievals on surface flux estimation, Geophys. Res. Lett., 41, 2598–2605, doi:10.1002/2013GL059174, 2014.

Thompson, D. R., Benner, D. C., Brown, L. R., Crisp, D., Devi, M. D., Jiang, Y., Natraj, V., Oyafuso, F., Sung, K., Wunch, D., Castaño, R., and Miller, C. E.: Atmospheric validation of high accuracy CO_2 absorption coefficients for the OCO-2 mission, J. Quant. Spectrosc. Ra., 113, 2265–2276, doi:10.1016/j.jqsrt.2012.05.021, 2012.

Wunch, D., Toon, G. C., Wennberg, P. O., Wofsy, S. C., Stephens, B. B., Fischer, M. L., Uchino, O., Abshire, J. B., Bernath, P., Biraud, S. C., Blavier, J.-F. L., Boone, C., Bowman, K. P., Browell, E. V., Campos, T., Connor, B. J., Daube, B. C., Deutscher, N. M., Diao, M., Elkins, J. W., Gerbig, C., Gottlieb, E., Griffith, D. W. T., Hurst, D. F., Jiménez, R., Keppel-Aleks, G., Kort, E. A., Macatangay, R., Machida, T., Matsueda, H., Moore, F., Morino, I., Park, S., Robinson, J., Roehl, C. M., Sawa, Y., Sherlock, V., Sweeney, C., Tanaka, T., and Zondlo, M. A.: Calibration of the Total Carbon Column Observing Network using aircraft profile data, Atmos. Meas. Tech., 3, 1351–1362, doi:10.5194/amt-3-1351-2010, 2010.

Wunch, D., Toon, G. C., Blavier, J., Washenfelder, R. A., Notholt, J., Connor, B. J., Griffith, D. W. T., Sherlock, V., and Wennberg, P. O.: The total carbon column observing network, Philos. T. Roy. Soc. A, 369, 2087–2112, doi:10.1098/rsta.2010.0240, 2011a.

Wunch, D., Wennberg, P. O., Toon, G. C., Connor, B. J., Fisher, B., Osterman, G. B., Frankenberg, C., Mandrake, L., O'Dell, C., Ahonen, P., Biraud, S. C., Castano, R., Cressie, N., Crisp, D., Deutscher, N. M., Eldering, A., Fisher, M. L., Griffith, D. W. T., Gunson, M., Heikkinen, P., Keppel-Aleks, G., Kyrö, E., Lindenmaier, R., Macatangay, R., Mendonca, J., Messerschmidt, J., Miller, C. E., Morino, I., Notholt, J., Oyafuso, F. A., Rettinger, M., Robinson, J., Roehl, C. M., Salawitch, R. J., Sherlock, V., Strong, K., Sussmann, R., Tanaka, T., Thompson, D. R., Uchino, O., Warneke, T., and Wofsy, S. C.: A method for evaluating bias in global measurements of CO_2 total columns from space, Atmos. Chem. Phys., 11, 12317–12337, doi:10.5194/acp-11-12317-2011, 2011b.

Yoshida, Y., Ota, Y., Eguchi, N., Kikuchi, N., Nobuta, K., Tran, H., Morino, I., and Yokota, T.: Retrieval algorithm for CO_2 and CH_4 column abundances from short-wavelength infrared spectral observations by the Greenhouse gases observing satellite, Atmos. Meas. Tech., 4, 717–734, doi:10.5194/amt-4-717-2011, 2011.

Yoshida, Y., Kikuchi, N., and Yokota, T.: On-orbit radiometric calibration of SWIR bands of TANSO-FTS onboard GOSAT, Atmos. Meas. Tech., 5, 2515–2523, doi:10.5194/amt-5-2515-2012, 2012.

Yoshida, Y., Kikuchi, N., Morino, I., Uchino, O., Oshchepkov, S., Bril, A., Saeki, T., Schutgens, N., Toon, G. C., Wunch, D., Roehl, C. M., Wennberg, P. O., Griffith, D. W. T., Deutscher, N. M., Warneke, T., Notholt, J., Robinson, J., Sherlock, V., Connor, B., Rettinger, M., Sussmann, R., Ahonen, P., Heikkinen, P., Kyrö, E., Mendonca, J., Strong, K., Hase, F., Dohe, S., and Yokota, T.: Improvement of the retrieval algorithm for GOSAT SWIR XCO_2 and XCH_4 and their validation using TCCON data, Atmos. Meas. Tech., 6, 1533–1547, doi:10.5194/amt-6-1533-2013, 2013.